Micro-Aerial Vehicle Design with Low Reynolds Number Airfoils

Francis Barnhart, Michael Cuipa, Daniel Stefanik, Zachary Swick

7th March 2004

Abstract

The goal of this project was to design, build and test a Micro-Aerial Vehicle (MAV) for competition in the 2002 International MAV Competition at Brigham Yound University. Topics researched include: gas and electric propulsion, low Reynolds Number aerodynamics, low aspect ratio wings, and micro radio controled electronics. Early comparisons of gas and electric propulsion systems indicated that an electric system would be more reliable, and weigh less at the cost of reduced thrust. An online airfoil database provided by the NASG was used to compare low Reynolds Number airfoils. From these comparisons the Wortmann FX60100 was chosen. Reasearch into low aspect ratio wing effects indicated that wing efficiency would be severly reduced and designs accounted for this. Light weight propulsion and control components were incorporated into the design. Common lithium batteries were chosen as the power source.

An iterative design process was used to generate several concept designs. These designs were refined as components were selected and aerodynamics analysis progressed. Analytical factors considered included: component placement and parameters, wing geometry, sizing, construction techniques, control surface size and location, center of gravity location, and tail placement.

The most promising concept design was fabricated. Windtunnel, lasso, and free flight tests were conducted to verify analytical results. Experimental results were used to further refine the design and augment the overall quality of the aircraft.

The final MAV design had a maximum dimension of 22.4 centimeters and a weight of 77 grams. The plane flew several short flights but was not completed in time for the 2002 MAV competition.

Contents

List of Figures

List of Tables

1 Notation

Below the meanings of symbols used throughout this report are indicated. Also, all calculations were conducted in standard SI units (Newtons, meters, etc). However, the resulting values were often converted to metric units that are commonly used to describe MAVs (grams, centimeters, etc).

V	Velocity
L	Lift
D	Drag
C_L	Lift Coefficient
C_D	Drag Coefficient
$C_{D,0}$	Parasitic Drag Coefficient
$C_{D,i}$	Induced Drag Coefficient
T	Thrust
η_p	Propeller Efficiency
e	Oswald Efficiency Factor
W	Weight
S	Wing Surface Area
b	Wing Span
c	Wing Chord
A	Aspect Ratio

α	Angle of Attack
λ	Taper Ratio
z	Largest Linear Dimension
p	Propeller Diameter
Re	Chord Reynolds Number
q	Dynamic Pressure
ρ	Air Density
μ	Air Kinematic Viscosity
x_c	Chord Location of Maximum Thickness
t_c	Thickness
E	Endurance
P	Power
v	Voltage
i	Current
C	Battery Capacity
η_m	Motor Efficiency

2 Design Process Overview

The design process was adapted from the general conceptual approach detailed in Raymer [8] and is pictured in Figure 1. The design process was highly iterative and drew on analytical theory which was later refined with experimental data. It began with the customary specification process. The rules of the 2002 Micro-Aerial Vehicle Competition provided a list of requirements and a scoring system for this step. Following the specification process several concept sketches were generated and refined as components, such as motors and servos, were considered. Promising concept and component combinations were analyzed with custom codes to determine their feasibility. Designs with the highest score were selected for integration and fabrication. Testing proceeded, first in stages where single design aspects, such as wing performance, were tested and later as complete packages that were subjected to lasso, durability, and flight tests. Throughout this analysis and testing process attention was given to flight performance aspects, including stability and controls, and the designs were further refined.

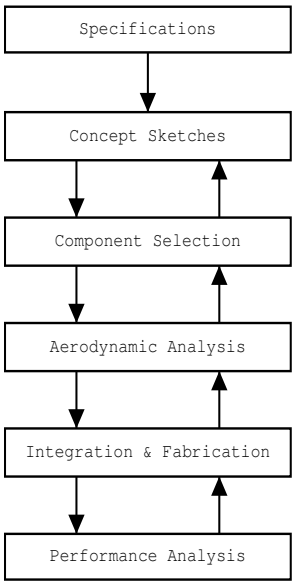

Figure 1: Design Process

3 Design Specifications

Specifications are adapted from the rules for the 2002 Micro R/C Competition [2]:

1. The objective is to build and fly the smallest Powered, Radio Controled (R/C) aircraft that can achieve the longest endurance. Launching by catapult is permitted.
2. The size of the Micro R/C is defined as the largest linear dimension, that is, the largest distance between any two points located on the Micro R/C while it is airborne.
3. If cables or antennas (except for the flexible R/C antenna) are used, which are connected to the Micro R/C while airborne, they will be included in the determination of the size of the Micro R/C.
4. Endurance is defined as the time from launch to landing for one continuous flight.
5. Vehicle must land within 100m of the launch site at the end of the flight.
6. For safety reasons, no pyrotechnics are allowed. Solar powered aircraft will not be allowed.
7. The event score will be calculated by dividing the endurance (in seconds) by the largest linear dimension (in centimeters) cubed. This scoring system places more importance on size. Score = endurance/(dimension)3 (sec/cm3).
8. The maximum endurance will be set at 900 seconds.
9. The vehicle with the highest score will be declared the winner.
10. The organizers reserve the right to clarify these rules at any time.

From these rules the following design specifications were derived:

1. Minimized largest linear dimension

2. Total weight under 100 grams
3. Endurance of 900 seconds
4. Nominal speed of approximately 12 meters per second
5. Stable in normal wind gusts
6. Operating altitude of approximately 1300 meters (the altitude of Provo, Utah)
7. Crash resistant

3.1 Mission

The mission was also based on the competition rules:

1. Takeoff
2. Climb
3. Loiter for up to 900 seconds
4. Land within 100 meters of takeoff point

3.2 Design Scoring

Designs were scored based on their largest dimension and endurance, as described in the 2002 Micro R/C rules:

$$\text{score} = \frac{\text{endurance in seconds}}{\text{largest dimension}^3} \tag{1}$$

This scoring method places the greatest importance on the largest linear dimension and the maximum endurance. Thus, the primary design considerations for our design process were:

1. Largest dimension

2. Endurance in seconds

4 Major Design Revisions

Due to the highly iterative nature of aircraft design many designs were considered. A summary of the major design revisions is given in Table 1.

Table 1: Major Design Revisions

Parameter	MAV-1	MAV-2	MAV-3	MAV-4
Date	October 2001	December 2001	March 2002	April 2002
Angle of Attack (deg)	8.6	12	12	9
Aspect Ratio	1.4	1.4	1.59	1.79
Chord (cm)	11.9	9.49	10.5	12.5
Drag Coefficient	0.0921	0.12	0.143	0.065
Endurance (sec)	900	900	-	15
Maximum Dimension (cm)	13.7	12.1	15.5	22.4
Lift Coefficient	0.402	0.31	0.590	0.391
Lift/Drag Ratio	4.4	2.58	4.13	6.0
Propeller Efficiency	0.75	0.60	0.33	0.39
Score	0.35	0.51	-	0.001
Span (cm)	12.9	11.44	14.8	21.8
Wing Surface (cm^2)	97.6	97.4	138	265
Taper Ratio	0.4	0.4	0.49	0.52
Thrust (gm)	13.7	8.42	8	12.8
Thrust/Weight Ratio	0.32	0.255	0.127	0.166
Velocity (m/s)	14	11.33	8.5	11.5
Weight (gm)	43.2	33.0	63	77
Wingloading (gm/cm^2)	0.44	.34	0.457	0.291

4.1 Initial Concepts

Several concept designs were generated and analytical analysis was applied to determine their expected performance. MAV-1 and MAV-2 were two of several such designs. They were based largely on assumptions based on historical data. Several of these assumptions were to prove lacking: propeller efficiency values were overly optimistic, battery performance was over estimated, and our weight estimate was too low.

Various planforms were also considered in the conceptual stage. For a Reynolds number of 70,000 the inverse-Zimmerman shape proved to be the most efficient at both aspect ratios. In the initial stages of construction, however, our group noticed that this type of planform would be difficult to create consistently, which would cause stability problems. The next best choice was the ellipse which performed extremely well with an aspect ratio of two but showed mediocre performance at a value equal to one. This was due to the ellipse being a circle at the lower aspect ratio; the flow doesn't separate around the circle and causes more drag. In the end, it was realized that the elliptical planform would be just as difficult to create as the inverse-Zimmerman so the resolution was made to construct the approximate elliptical shape that can be seen in the final design.

4.2 Experimental Designs

The aircraft went through a number of major deign revisions necessitated by problems that were encountered during testing and analysis. The first models were built for testing in the wind tunnel. One of the first things explored was whether a cambered plate would perform as well as a full airfoil. Both were tested to make a comparison of how they performed. These were made entirely out of balsa wood ribs and transparency film for a covering. See Figure 2 and Figure 3 for examples of the cambered plate and the first full airfoil design, respectively. From the tests it was determined that the full airfoil would be more efficient than the cambered plate and future designs would employ a full airfoil.

Next preliminary stability tests were conducted on the full airfoil using Pro/Engineer drawings. At this point a single CR2 was used as a power source for the WES-Technik DC5-2.4 motor. A problem with construction was that folding transparency over the corners of the leading edge created holes and serious inconsistencies. Since the leading edge of the wing is very crucial to lift, roll, and drag it was decided to explore another construction method.

Instead of completely changing the construction method, the team decided to continue

Figure 2: Cambered Plate

Figure 3: Full Airfoil — Balsa and Transparency Constuction

using the transparency over balsa design, and modified the wingtips of the plane. The wingtips were made out of polystyrene and attached to the center section on either side. This reduced some of the major inconsistencies in the leading edge but did not entirely eliminate irregular drag issues. This aircraft, in figure4, had also increased in size slightly at this point and was slightly underpowered because of increased drag and weight, therefore a second CR2 was added to increase the thrust. The elevons were also moved to the center section in order for wingtips to remain expendable. Roll problems existed with this construction type, due to warping in the transparency. The amount of roll was too extreme to be corrected with the control surfaces.

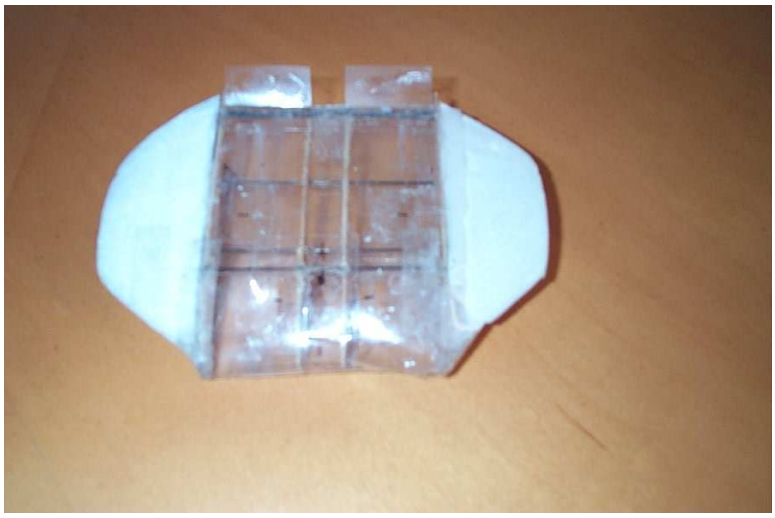

Figure 4: Hybrid Constuction

MAV-3 was the first model built by the group that was made entirely out of polystyrene foam. This construction method was adopted due to the warping in balsa models. Three sections where constructed by cutting then sanding: a straight center section and two tapered wingtips. The model had an area of 138 square centimeters, with the same elevon and flap arrangements as the previous models. Early lasso tests of this model indicated that it did not have enough control surface to climb well, therefore the size of the control surfaces was doubled by gluing thin plastic sheets over the existing flaps. The first free flight tests of the model indicated that the pilot was capable of trimming the plane level for roll after

several tests. At this point the plane flew several short level flights, but did not have enough power to climb. It was determined that the plane did not have enough lift for the amount of propulsion and needed to be scaled up. MAV-3 can be seen in Figure 5.

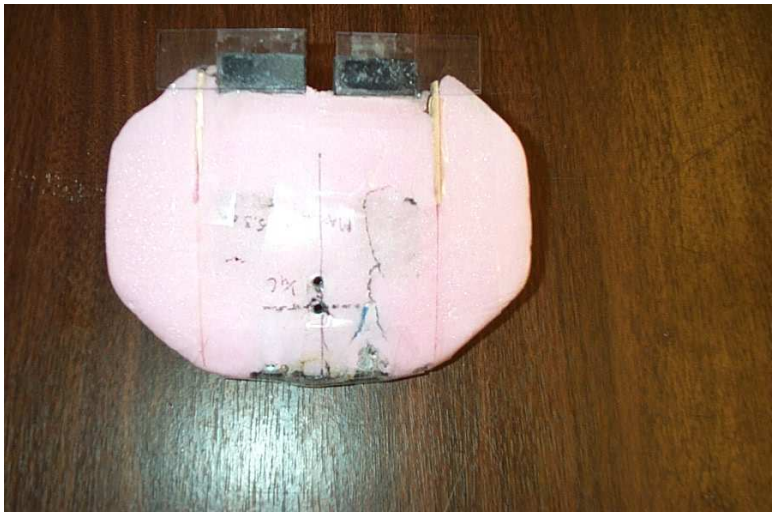

Figure 5: MAV-3

4.3 Final Design

The group built MAV-4, shown in Figures 6 and 7, to ensure that enough lift was produced. While this was accomplished, the extra drag produced by the large wing was detrimental. Early flight tests of MAV-4 with two CR2 batteries did not provide enough thrust. A 6 second flight test was attained with this configuration, but it was clear the plane was continually losing altitude. The group then chose to add a third CR2 battery to the propulsion system in order to increase the voltage to the motor and gain thrust. With a third battery the plane flew significantly better with several flights of approximately 15 seconds. The plane had enough power to climb and the pilot could keep the plane in the air as long as he flew straight. Upon attempting turns, however, the plane would rapidly roll and slide from the sky. This severely limited endurance. The control surfaces were determined to be too close to the center line of the plane, not allowing for the pilot to rescue the plane from a sharp

roll.

Key features of the final design include: A larger than anticipated lift-to-drag ratio. A uniform construction method. Twin balsa, vertical tails mounted under the wing. Three CR2 batteries and a WES-Technik DC5-2.4 for a power output of 4 Watts that, combined with a U-80 propeller acheived a flight thrust of 23 grams. A Sky Hooks & Rigging RX72 receiver was used in conjunction with WES-Technik Micro 2.4 servos for the controls system. To protect the receiver, a voltage regulator was utilized to reduce the voltage to the receiver from 8 to 5 volts. To reduce drag the stock RX72 antenna was replaced by a custom, coiled antenna that required less wire to be exposed to the free stream. The linear servos employed were contected to the elevons via sections of piano wire. The linkage system and servos were protected by the vertial tails and plastic servo covers during crashes. Components mounted in the wing were covered with clear packaging tape to reduce drag.

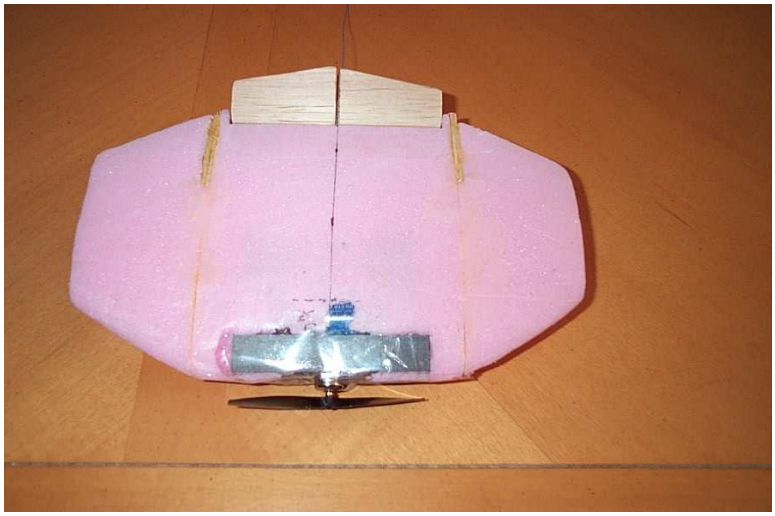

Figure 6: MAV-4

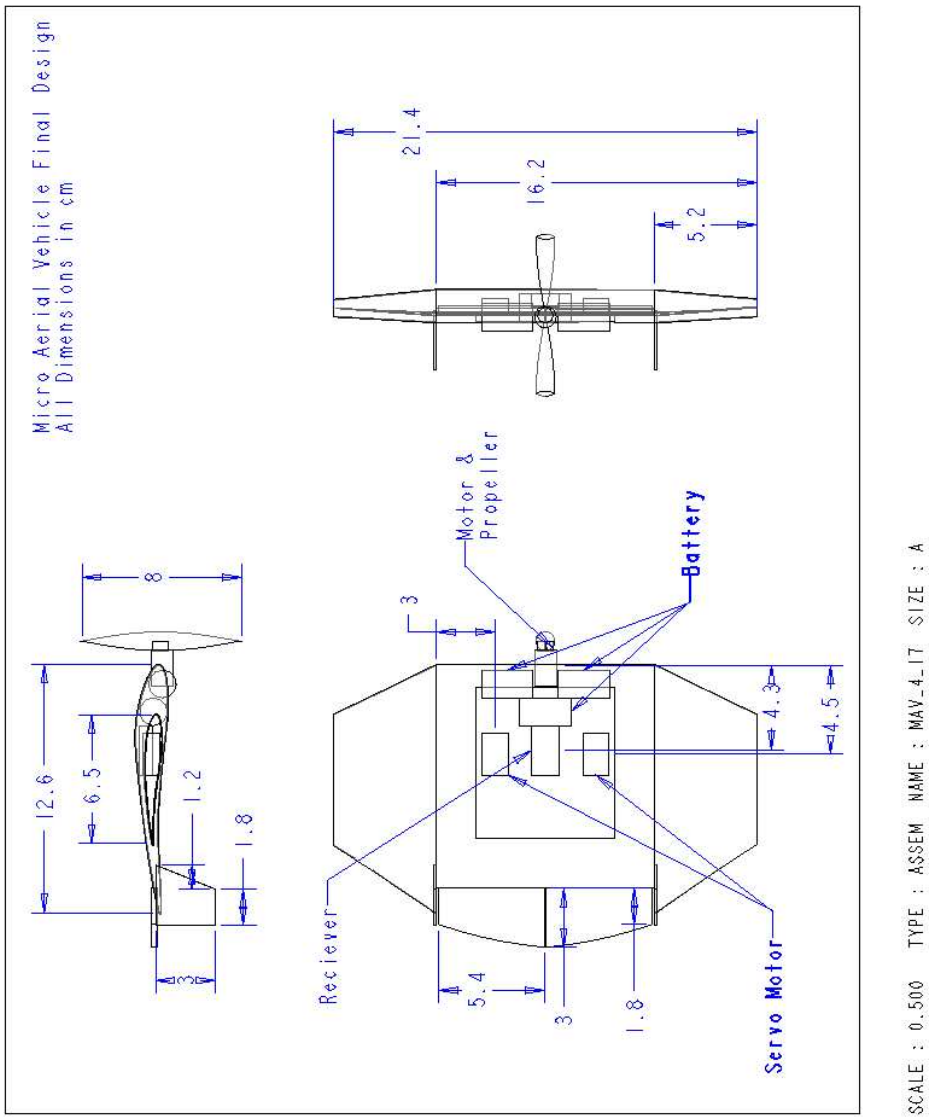

Figure 7: MAV-4 Three View

5 Background

A Micro-Aerial Vehicle, or MAV, is the smallest in the category of unmanned-aerial vehicles, UAVs. The general definition of an MAV is a UAV with a largest linear dimension of no more than six inches. MAVs are intended for use in close proximity to a target area by surveillance teams to quickly gather critical information without being detected. Some possible missions for an MAV are reconnaissance, and biological or chemical agent detection. MAV research is currently being conducted by commercial interests, government agencies and educational institutions.

5.1 Historical Overview

The Black Widow is the current state-of-the-art MAV and is an important benchmark. It is the product of 4 years of research by Aerovironment and DARPA. The Black Widow has a 6-inch wingspan and weighs roughly 56 grams. The plane has a flight range of 1.8 kilometers, a flight endurance time of 30 minutes, and a max altitude of 769 feet. The plane carries a surveillance camera. In addition it utilizes computer controlled systems to ease control. The Black Widow is made out of foam, indiviual pieces were cut using a hot wire mechanism with a CNC machine allowing for greater accuracy. The multi-piece construction and the final design can be seen in Figure 8.[3]

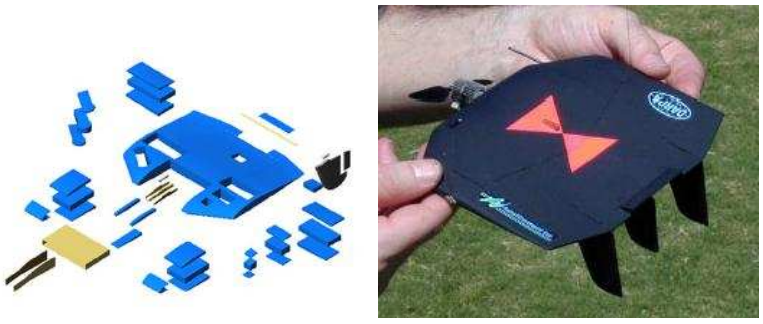

Figure 8: Black Widow

In 2001 there were two MAV competition categories. One was a heavy lift competition

in which the MAV was required to carry a 2 oz. payload. The other competition was a micro surveillance competition in which planes had to fly by video camera to a target area, photograph the target, and return to the launch site.

The University of Florida has has been very successful over the past five years in the MAV competitions. In 2001 they won in both the heavy lift and surveillance categories. Their plane was constructed of a resilient plastic attached to a carbon fiber web structure. This resutled in a crash resistant airfoil. Florida's design philosophy centered around the 90 grams of thrust produced by the COX TEE-DEE .01 internal combustion engine. Figure 9 shows a picture of the University of Florida design for the heavy lift competition. [16]

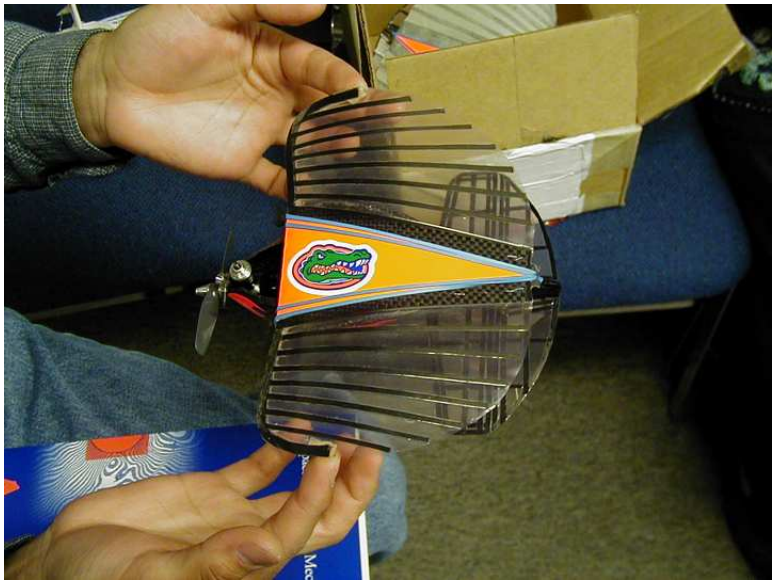

Figure 9: University of Florida 2001

Notre Dame's MAV design was entered in both the heavy lift and the surveillance competitions also. The plane was constructed out of balsa and foam. It should be noted can also see that the design has a large fuselage, which would increase the drag greatly, however this design also utilized the COX .01 TEE-DEE. Control was provided by an airleron/elevator system mounted below the wing and a rudder on a vertical tail above the wing. The Notre Dame design can be seen in Figure 10. [17]

Brigham Young University has been involved with the MAV competition for a num-

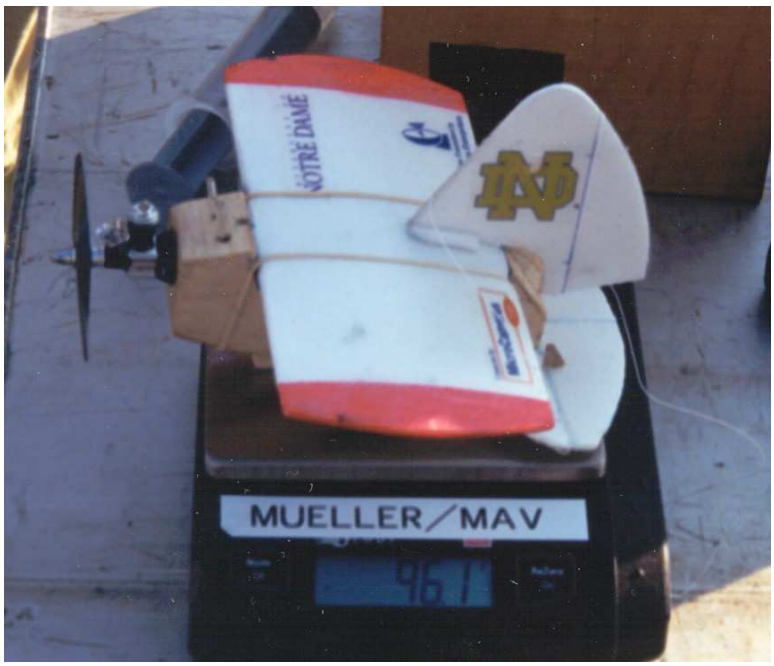

Figure 10: Notre Dame 2001

ber of years now, and their concept has been different. They have chosen to increase the wing area without increasing their largest dimension by making a biplane. The two wings double the surface area without affecting the maximum dimension of the aircraft. Another technique that was employed by the Brigham Young team was to bring multiple planes to the competition. Some of these planes were much larger than others. The idea behind this was that the large plane could be flown to guarantee a qualification for ranking, and once that was done, they would attempt to make their smaller planes fly for the necessary two minutes to qualify. Figure 11 shows some of the MAVs that were designed by Brigham Young. [18]

Arizona State University has also been involved with the competition for a number of years. Their design featured a simple swept, flying wing design. It also uses the COX .01 TEE-DEE engine for thrust. The control surfaces are at the trailing edge of the wing, and it uses an aileron system for turning. [19]

The 2001 MAV from Worcester Polytechnic Institute placed 4th in the 2001 compe-

Figure 11: Brigham Young 2001

tition. Their plane was constructed out of a carved block of polystyrene. The electric propulsion system, control system, and payload were stored in a rectangular fuselage below the wing. The team also used a folding propeller to gain an advantage on its maximum dimension. The rules have since been changed to stipulate that the largest dimension is measured in the flight condition.[20]

There are some similarities in many of these aircraft. Almost all of the designs use the COX .01 TEE-DEE engine. Almost all of the designs also use a leading edge that is swept back from the propeller, which allows for a slightly more efficient thrust from the engine, or motor. Table 2 contains some of the important values of a few MAVs that have been flown in the recent past.

5.2 Aircraft Planform

The planform and aspect ratio of an airfoil have been shown to effect airfoil efficiency on large scale craft; they will determine how a wing is affected by common losses of in efficiency like wingtip effects and viscous skin drag. These effects can be seen in small

Table 2: Historical Data

Parameter	U. of Florida	Notre Dame	Black Widow	WPI
Year	1998	2000	1999	2001
Wing loading (gm/cm^2)	0.38	0.186	0.314	0.70
Total weight (gm)	283	105	56.5	354
Max. thrust (gm)	340	90	9.4	157
Velocity (m/s)	11.2	11.2	11.2	15.65
Aspect ratio		1.5	1.29	1.35
Wing area (cm^2)	745	516	180	509
Lift coefficient		0.55	0.42	0.53
Drag coefficient		0.18	0.07	0.08
Angle of attack (deg)		12		
Max. dimension (cm)		21.6	18.2	31.75
Lift/drag ratio		3.14	6.0	2.13

aircraft applications as well. However, as the Reynolds number decreases and drag effects begin to overcome other aerodynamic properties, the losses of efficiency are magnified. For this reason much planning and research has been done to determine the best choice of aspect ratio and planform for MAVs.

In order to maximize the largest dimension for our aircraft we were limited to low aspect ratios in the range of one to two. Historical data from previous MAVs pointed our group in the direction of an aspect ratio 1.4 to 1.5. This range is highly susceptible to losses in lift due to flow slip near the wingtips. Torres and Mueller show that in the Reynolds number range between 60,000 and 120,000 where most MAVs travel there is a decrease in lift curve slope that is directly related to the aspect ratio of the wing. This decreases the overall efficiency of the low aspect wing because the angle of attack must increase to provide the same amount of lift as an airfoil with greater aspect ratio. Therefore the low aspect ratio airfoil has higher drag coefficients for matching lift coefficients of larger aspect wings. After using finite wing theory to estimate the losses for the 1.4 to 1.5 aspect ratio range and weighed these versus the loss in score due to an increase in the craft's maximum dimension, the decision was made to follow historical data.

5.3 Component Drag

At low Reynolds numbers drag becomes and large factor in whether a plane will become an aircraft or just a test model. For this reason it is important to consider all factors of drag in micro air vehicles. Although, the efficiency of the wing is covered in the airfoil selection there are other sources of drag to be considered on most small aircraft. Two major components which can be a cause for concern are vertical tails and fuselage-like structures. These two external components of the aircraft may be necessary for stability and internal component placement. Their effects, however, can be minimized through proper optimization.

Vertical tails on small flying wings are used mainly to provide roll stability. The roll rates of these small aircraft are extremely fast, so keeping them moving fairly straight tends to be the best choice. These tails then become necessary losses that must be accounted for. Tails can be optimized minimizing the area enough to provide the proper amount of stability with the least possible amount of drag. For this aircraft we were limited by the largest linear distance between any two points on the craft in three dimensions. This stipulation left the group with no choice but to assure that the ends of the tails didn't create the largest dimension themselves.

Though tiny airfoils can be constructed from paper, it doesn't mean that they will be controllable aircraft. Currently, stock internal components such as servos, batteries, and propulsion systems can not fit into the airfoil thickness of most micro air vehicles. Fuselages are thus used to cover these components and decrease the drag that is created by them. Fuselages, however, are not drag free, and if care is not taken in component placement the gains provided by a fuselage may be offset by the weight it adds. Ramamurti and Sandburg show that the addition of any fuselage to a pure airfoil will cause losses in lift, increases in drag, and therefore an overall decrease in efficiency. Since components must be placed to create stability in the aircraft, the process of optimization isn't that simple. Experimental results for drag on three dimensional bodies which can be found in most fluid mechanics

textbooks show that the optimal shape for a fuselage would be an ellipsoid. As the ellipsoid becomes longer and thinner relative to the freestream flow there is a decrease in drag on it in both laminar and turbulent flows. Examples of these results can be found in White's undergraduate text. Several attempts were made to produce a fuselage for our small craft with little success. Stability, component placement, and time became the limiting factors in the design of a specialized fuselage for our craft. The components were generally covered with a material that provided a smoother surface which created a blended wing type effect.

6 Component Selection

6.1 Airfoil

Generally between eight and sixteen centimeters in chord length, with flight speeds of six to twelve meters per second, MAVs fall within a Reynolds number (Re) range of 50,000 and 120,000, in which many causes of aerodynamic effects are not fully understood. The research field of low Re aerodynamics is currently an active one, with many universities (e.g. Norte Dame, Brigham Young University, University of Florida) and corporations working towards a better understanding of the physical processes of this aerodynamic regime.

Though the causes of many of the aerodynamic effects that occur at low Reynolds numbers have not been realized, we do know what some of the effects are. In this range of low Re, laminar flow is achievable, though at a very weak level. The problem with the weakness is that if laminar flow boundary separation occurs at these Reynolds numbers we often see "bubble" formation which can cause turbulent flow that will not reattach to the airfoil. This will cause a dramatic loss in lift for any airfoil and create an unwanted stall effect. Apart from this decrease in lift we also see increases in viscous skin drag with decreasing Reynolds numbers. This decreases the efficiency (L/D) for wings and tends to cause most airfoils to become inefficient at a Re below 50,000 [24]. However, we still see flight at lower Reynolds numbers as in so-called "creep" flows with orders of magnitude in the hundreds, where insects fly. In fact, at lower Re, a flat or cambered plate will out perform a traditional, thick airfoil because of its sharp leading edge as Laitone shows in his article [25]. In the range of our consideration however, we see a transitional range where either type may excel. Therefore, the difficulty in our airfoil selection lay in choosing the airfoil that was best for our specialized needs.

The group set required aerodynamic specifications for the specialized airfoil that we would use on our aircraft:

- High Lift to Drag Ratio (high efficiency) in our Re range

- Relatively Calm stall effect

The group decided on using a cambered plate airfoil which would have approximately the same camber as the thick airfoil that we chose so that experimental comparisons between the two could be drawn. From these comparisons a decision could be made on whether to use a cambered plate or a thick airfoil. However, we needed to find a good selection of full thickness airfoils to investigate and compare before making our final decision. Although, we had several airfoil catalogues on hand to choose from, most airfoils are not suitable for use at these lower Re values. When decided to check the internet for available catalogues dealing with airfoils specifically for the use of low Re flight. Fortunately, the Nihon University Aero Student Group (NASG) has an online airfoil database that is updated by engineers everywhere with experimental data for these types of airfoils [22]. Though the NASG's primary research focus is human powered flight, our Reynolds number ranges overlap, and the information that we gathered from their website allowed us to choose four airfoils for further investigation. These airfoils were the NACA 25411, the Eppler E193, the Gilbert Morris GM15SM, and the Wortmann FX60-100.

These four airfoils cover a good range of camber, thickness, and leading edge radius as can be seen in Table 3. We felt that this would give us a feasible test group as well as offer us a greater understanding of how these physical characteristics affect airfoils in our Re range.

Table 3: Physical Characteristics of Selected Airfoils [22]

Parameter	NACA 25411	E193	GM15SM	FX60100
Thickness	0.1100	0.1023	0.0674	0.0999
Camber	0.0250	0.0354	0.0476	0.0356
LE Radius	0.0133	0.0087	0.0046	0.0069
TE Angle	14.5600	5.5406	20.9478	5.2198

The NACA 25411 airfoil was designed as part of the second generation of NACA airfoils. We know this from the five number designation system that was used on this series of

airfoils. We see that it has the largest thickness and the least amount of camber of the four chosen airfoils, which, according to Laitone, should provide the least performance. The shape of the airfoil can be seen in Figure 13.

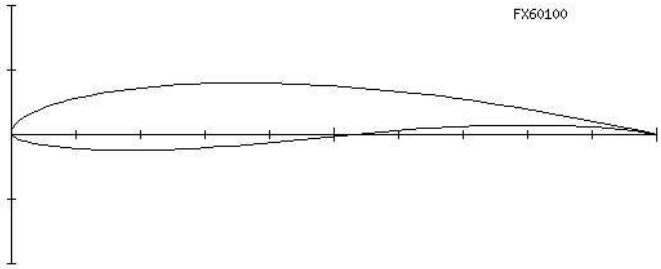

Figure 12: Wortmann FX60-100

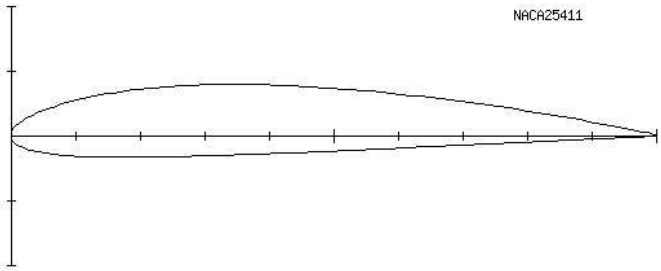

Figure 13: NACA 25411

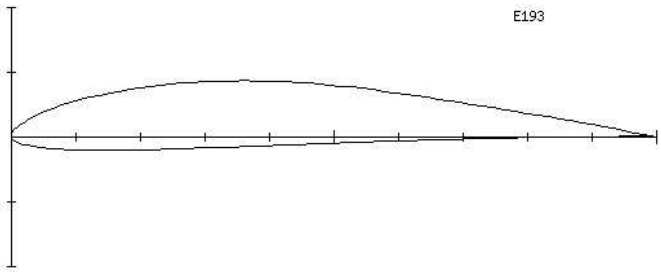

Figure 14: Eppler E193

Eppler's E193 airfoil shows less thickness, greater camber, and a smaller leading edge radius than the NACA airfoil. These were the key features that we were looking for from an airfoil based on research. The Wortmann FX60-100 has similar characteristics to the

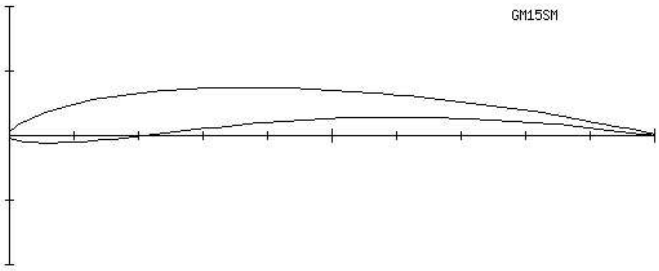

Figure 15: Gilbert-Morris GM15SM

Eppler, except that its leading edge radius is slightly smaller. This should lead to greater efficiency. However, there was an airfoil with a greater amount of camber and smaller thickness that had the potential to out-perform all of the others; the Gilbert-Morris had approximately a 1% greater camber than the two closest and had the smallest leading edge ratio of all. To determine the final choice, the group looked at the polar graphs for each airfoil at Reynolds Numbers of 100,000 and 60,000 (approximately). These can be found in Figure 16 and Figure 17, respectively. It is plain to see that the NACA airfoil is nowhere near the performance of the other airfoils at the lower Re. However, it does begin to catch up to the pack as the Reynolds number increases. The Eppler and Wortmann have very similar efficiencies as was expected due to their similarities. However, we can see that in both cases the Eppler has a large increase in drag before the maximum lift point is reached. This could have caused stability issues in our small craft so we discarded the E193 from the selection process. With the Wortmann and G-M airfoils left we had to examine them two more carefully. The polar graphs show similar response at higher Re, but at the lower the lower Reynolds number the GM15SM is more efficient than the Wortmann. However, the decreased thickness of the GM15SM would cause a greater increase in drag once the components were all placed into the airfoil. We also noticed that the stall characteristics of the G-M were much more erratic than those of the Wortmann. Therefore, with future considerations in mind we chose the Wortmann FX60-100 as the thick airfoil that best suited our needs.

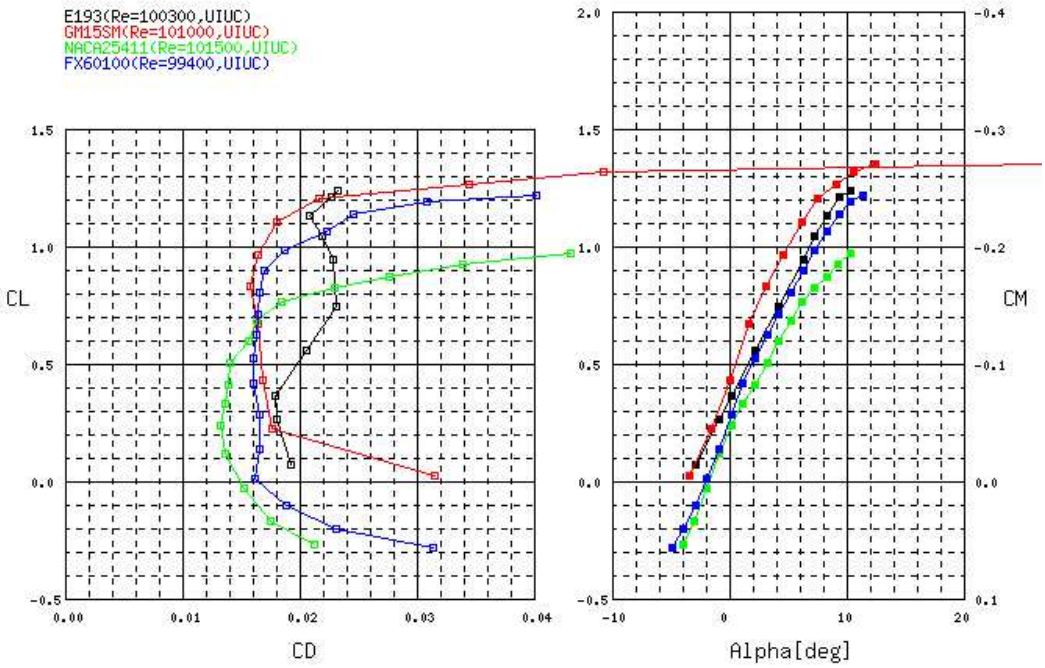

Figure 16: Airfoil Polars (Re=100,000) [22]

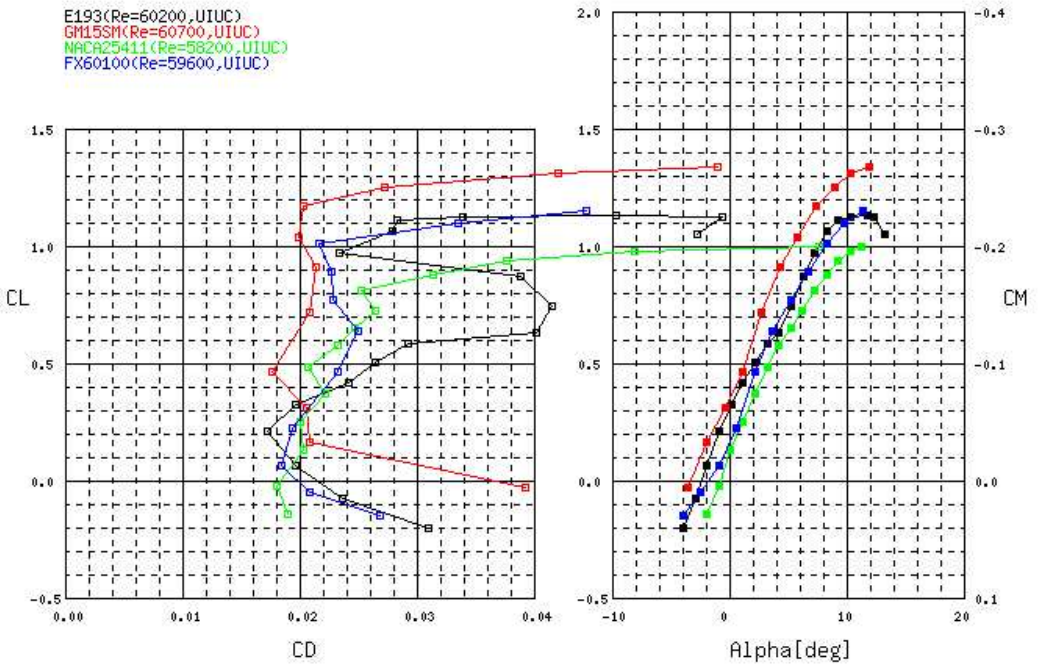

Figure 17: Airfoil Polars (Re=60,000) [22]

After selecting the thick airfoil that appeared to be the preeminent choice for our purposes, we built a test model using it. In addition there was a cambered plate airfoil which used the upper surface of the Wortmann profile as a guide. These two airfoils were tested in the wind tunnel at an approximate Reynolds Number of 90,000, which coincided with our estimated flight velocity. Though these tests were marred with errors due to our initial issues with the tunnel, we found that the Wortmann airfoil would be the best choice for out uses because it had better overall efficiency than the cambered plate.

6.2 Motor

Early on the decision was made to pursue electric propulsion over an internal combustion engine. Preliminary calculations of fuel consumptions for the smallest available combustion motor, the COX .010, indicated that endurance would be low for an aircraft of our size. Furthermore, an electric solution has the weight advantage of powering all components off one common power source. In addition, an electric motor is more reliable and does not pose the difficulties of a moving center of gravity caused by an emptying fuel tank.

Several motor sources were considered, including: micro-R/C motors commonly available through hobby shops and commercial motors from manufactures such as Smoovy and Farhauber. Micro-R/C motors have a larger power output than the commercial motors we considered but at the cost of increased weight. Since utilizing one of the commercial motors would not have allowed a reduction in battery weight the WES-Technik Micro DC5-2.4 was selected. Several of the motors considered are shown in Table 4. Values were calculated using the following relations for the mechanical output power:

$$P = vi - i^2R \tag{2}$$

and the efficiency:

$$\eta_m = \frac{P}{vi} \tag{3}$$

Table 4: Motor Comparison

Parameter	WES-Technik Micro DC5-2.4 [9]	Smoovy SYV88001 [10]	Faulhaber 1224 006 S [11]	Faulhaber 1319 006 S [12]
Voltage (V)	5	6	6	6
Current (A)	0.9	0.26	0.32	0.38
Resistance (Ω)	2.7	7	6.6	6
Power (W)	2.31	1.09	1.25	1.41
Speed (RPM)	21000	13500	13700	16300
Efficiency $(\%)$	51.3	69.9	65.1	61.8
Weight (gm)	10	5	13	11

6.3 Batteries

Most R/C vehicles use rechargeable nickel cadmium(Ni-CAD), nickel zinc(Ni-Zn), or nickel metal hydride(Ni-MH) batteries because of their high current draw, long life and very slight recharge memory. Rechargeable batteries are preferred for this type of application because they are cost effective and would not need to be removed from the plane. However these batteries are very heavy and are designed for long life. Our application required that a battery have a high continuous current draw with a relatively low capacity due to the fact that we were only running for 15 minutes. Table 5 shows a comparison of some sample batteries for the reason of comparing different battery chemistries only.

As can be seen in the table lithium batteries have a higher power density $(W \cdot hr/kg)$ than other batteries. Lithium seemed to have many of the qualities necessary for an MAV and there were several different models in the correct size range. Lithium polymer rechargeable cellular phone batteries were researched and explored but were not attainable for this project. This was due to manufacturer's insistance that they needed to verify our circuitry

Table 5: Battery Chemistry Comparison [13]

Parameter	Li-Ion	Li-Metal	Ni-CAD	Ni-MH	Ni-ZN
Manufacture	BYD	Tadiran	BYD	Varta	Evercel
Type	AA	AA	AA	AA	Box
Nominal voltage (V)	3.6	3	1.2	1.2	1.65
Nominal capacity $(A \cdot hr)$	0.75	0.8	0.9	1.3	39
Nominal capacity $(W \cdot hr)$	2.7	2.4	1.08	1.56	64.4
Usable cycles	600+	700	800+	1000+	500+(2)
Power denisty $\left(\frac{W \cdot hr}{kg}\right)$	135	141	47	70	59
Power density $\left(\frac{W \cdot hr}{L}\right)$	365	325	142	213	91
Max. discharge rate(A)	1.5	10	18	3.9	115

for safety reasons prior to any purchase. The manufacturers also required bulk orders of hundreds of units.

The ideal batteries would fit completely inside the wing of the MAV. To fit inside the wing the battery would need to be very thin, less than 8mm in one dimension. The only batteries of that size and shape did not meet the electrical requirements of the motor. Custom batteries were researched but did not fit within the budget or time frame of this project.

Many electronic devices use lithium batteries of other sorts such as CD players, MP3 players, and digital cameras. The batteries for these devices are sold in most electronics stores in many sizes, shapes and voltages. Most all of these batteries are cylindrical with some being small enough to fit completely inside the wing of an MAV. Common lithium camera batteries offer the most continuous current draw. These batteries are available in 3 and 6 volts with different sizes and capacities. The CR2 camera battery was found to perform the best with the chosen DC motor and was eventually used in sets of 2 and 3, in series. The specifications of the CR2 battery are show below in Table 6, a comparison chart of several "off the shelf" batteries.

Table 6: Battery Comparison

Battery	Chemisty	Nominal Voltage (V)	Max Continuous Current (mA)	Capacity $(mA \cdot hr)$	Mass (gm)
Energizer 123	Pile Li-Ion	3	1500	1300	15.5
CR2 *	Pile Li-Ion	3	2000	750	11
Energizer L544	Li-Ion	6	400	190	9
Duracell 28A	Alkaline	6	250	~200	9
Radio Shack 1/3N	Lithium	6	400	160	8.5
Duracell MN175	Alkaline	7.5	300	~400	9
LR44 Button Cell	Alkaline	1.5	350	~50	1.9
Tekcell AA	Lithium	3.6	200	2200	14.2
Tadiran 1/2AA	Lithium	2.6	150	1000	9

* CR2 batteries made by Energizer, Duracell, Radio Shack, and Sanyo were tested, all specifications were nominal.

6.4 Propeller

6.4.1 Geometry

There are two dimensions that are used to describe propellers, diameter and pitch. These two dimensions can be seen in Figure 18 below. Diameter is simply the length from tip to tip of the propeller.

The pitch is the length the propeller would move forward in one revolution in an ideal fluid. It can be explained as similar to the wavelength of a wave, the distance moved in one cycle, as shown in Figure 18. The pitch of the propeller is dependent on the angle of twist of the blades on the prop. On most propellers however the angle of the blades changes with the position on the radius of the prop. Therefore the measurement of pitch listed for a propeller is and average of the changing blade angle, and for most R/C applications is only an estimate. [21]

6.4.2 Characteristics

The propeller supplies the thrust for the propulsion system. The thrust that is created by the propeller is difficult to predict because there a several inter-related parameters that effect

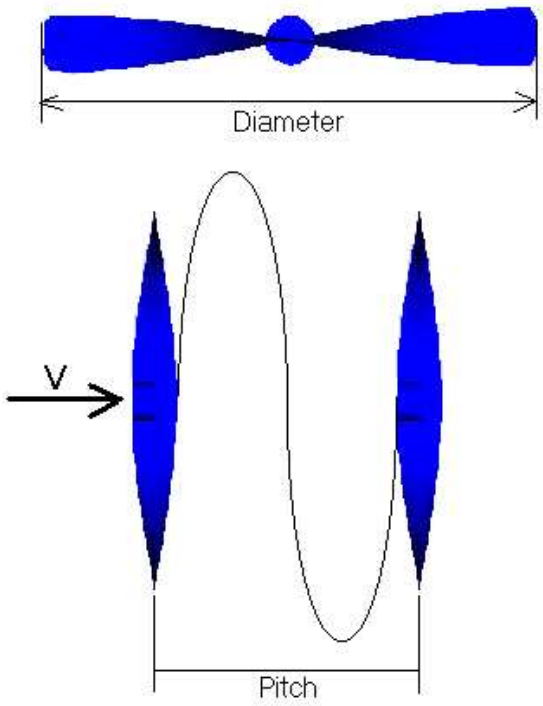

Figure 18: Schematic of Propeller Dimensions

the thrust. Parameters include are prop dimensions, flow speed, prop angular velocity, air density, and prop efficiency. The dimensions of the propeller in R/C applications are fixed, as is the air density, therefore the parameters that a designer can affect are flow speed, prop rpm and prop efficiency, all of which are dependent on each other. The equation for propeller efficiency is:

$$\eta_p = \frac{VT}{P} \tag{4}$$

Where V is the plane velocity, T is the output thrust, and P is the power output of the motor. This value can only be attained experimentally because the thrust output and velocity are dependent on each other through the drag of the plane and also the prop dimensions and rpm. The rpm of the propeller is dependent on both the power of the motor and the velocity of the flow.

Typical R/C propeller efficiencies are lower than full-scale planes, generally in the range of 25-80%. The efficiency is lower due to manufacturing limitations set by the low cost of these propellers. Most propellers are not optimized for the plane/speed at which they fly. Finding the right propeller for a particular design can be quite difficult.

6.4.3 Testing and Selection

Every propeller on the R/C market is optimized for one of the parameters mentioned. Many are designed for specific motors, or rpm, while others are designed for specific size planes. The problem is that most R/C catalogs are not explicit (or are ignorant) regarding the design parameters of the props. This necessitates experimental testing in selecting a prop for a plane. At the start of the component selection process for this project the propeller selection was driven by both the weight and diameter, which affect the maximum dimension of the MAV. When motors were first purchased for the MAV, several different propellers, in the correct size range, were also purchased for testing.

Initial qualitative testing was done on several propellers running on the micro DC5-2.4

motor, with and without a gear unit. Three propellers were initially tested: the Union U-80 8x2.2 cm, a 15X6cm (P1), and a 14X4.5cm (P2). Due to the time frame of the later part of the project not all of the information gained during the propulsion testing could be implemented. P1 had a higher propeller efficiency than the U-80. However, the U-80, with three batteries, was chosen because it produced the required thrust. Figure 19 shows the thrust for the U-80 propeller vs. velocity of the free stream. Propeller efficiencies are included on the graph as well.

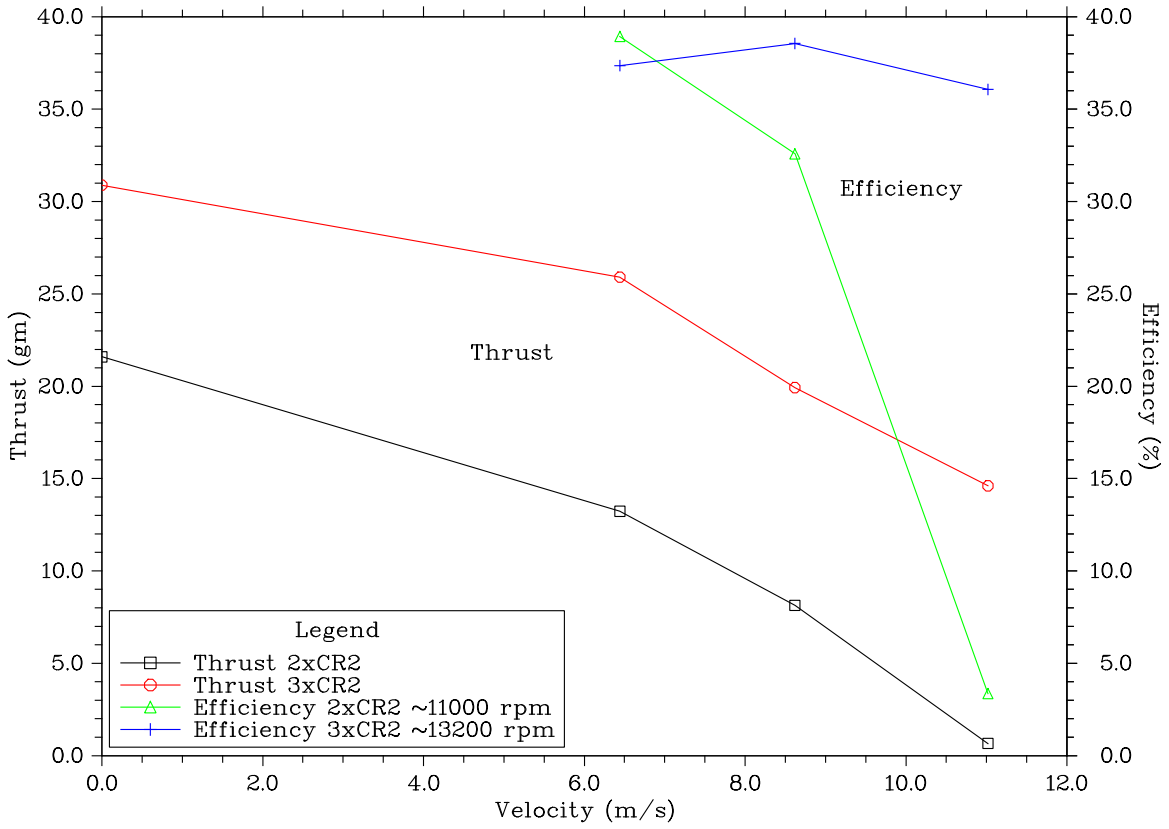

Figure 19: U-80 Ungeared Propeller

As can be seen in Figure 19 the efficiencies for the 2 battery configuration are 38% at 6.4 m/s, 32% at 8.6 m/s, and 3.4% at 11.3 m/s. While the efficiencies for the 3 battery configuration were 37% at 6.4 m/s, 38% at 8.6 m/s, and 36% at 11.3 m/s. It should be noted that the efficiencies of the propeller, with different battery configurations, at the slow

speed is very similar, whereas at the higher velocities the efficiency of the prop with three batteries goes up significantly. The 3-CR2 battery configuration is the one with which the MAV flew; however the highest efficiency was only 38%. This is a relatively low efficiency for even an R/C propeller, and should be improved in future MAV designs.

Figure 20 shows the graph of thrust and efficiency for geared systems that were tested. The main thing to note from this plot is that while the thrust given by the props are much less than the U80/3CR2 combination at 6.4 and 8.6 m/s, the efficiency for P1 is much higher. P2 had an efficiency of 50% at 6.4 m/s, 26% at 8.6 m/s, and negative (due to propeller drag) at 11.3 m/s. While the efficiencies for P1 were 56% at 6.4 m/s, 54% at 8.6 m/s, and 17% at 11.3 m/s, the highest of the tested systems.

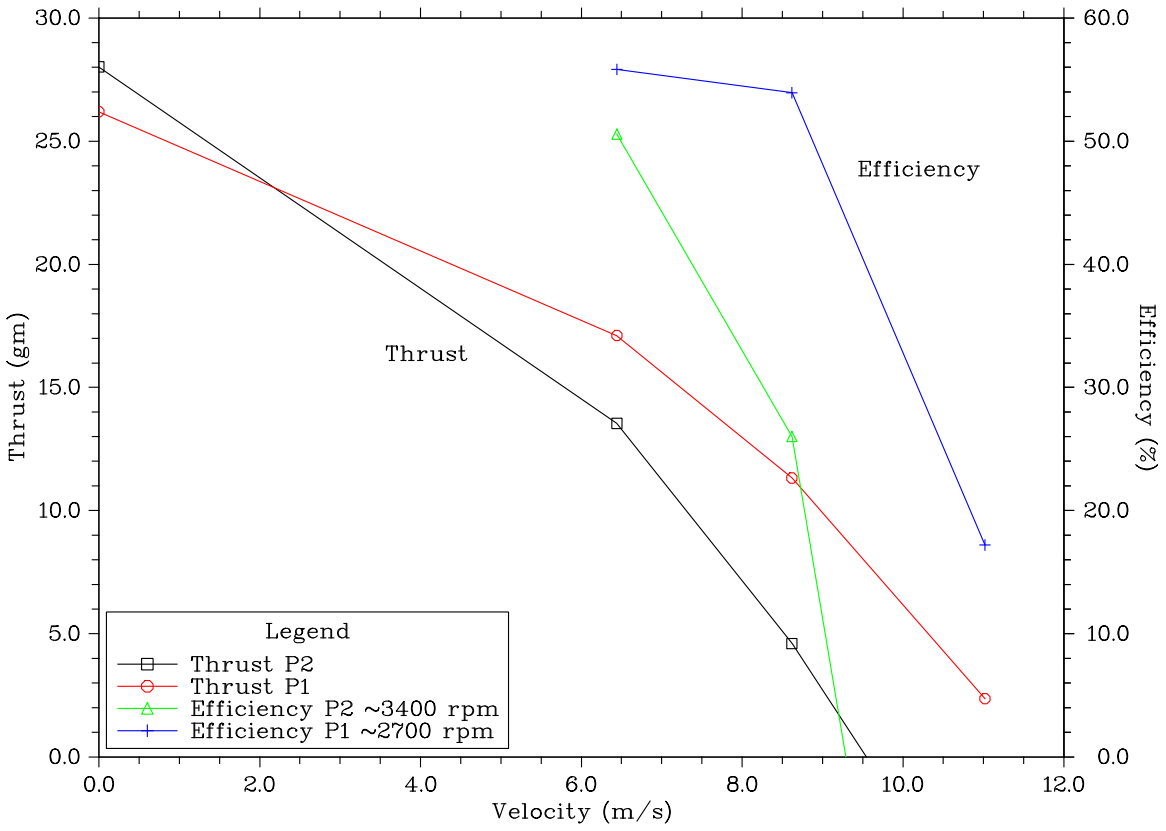

Figure 20: Geared Propeller Comparison

Even though P1 was more efficient than the chosen system, it did not provide the re-

quired thrust with 2 or 3 batteries, and could not be used. In the future extra effort should be spend on getting the most efficiency out of the propulsion system of the MAV. This is where a huge potential in weight savings and size could be found.

6.5 Receiver

A receiver is the part of the plane that receives the information from the pilot controlled transmitter. Receivers have an antenna attached to them and also have a power input plug and output plugs to the servo flap controllers. The type of receiver required by the Hi-Tec transmitter, was FM channel 37. The R/C supplier Sky Hooks and Rigging was the leading manufacturer of sub-micro receivers. A chart of the many receivers for sale in the weight range required by this MAV is show below as Table 7. The chart has seven different models that are quite small. The weight was the most important parameter to the design, providing the receiver was compatible with the transmitter. Some of these receivers have a speed controller built into them for controlling the motor speed. These receivers are called hybrid receivers and are labeled in the chart HYB. Speed controllers are not entirely necessary for a model plane but do allow the pilot to "throttle back", which can save battery life significantly.

The lightest receiver in the table, the RX-72, was the model chosen for the MAV. This receiver had all of the necessary requirements and was chosen for it’s small mass.

6.6 Antenna

The antenna that comes with an R/C receiver is usually a 39 inch light wire antenna soldered to the receiver. This antenna is designed to hang off the back of the plane and receive the communications. It seemed however that this type of antenna would create a noticeable drag force at this scale of aircraft. For that reason alternate antenna designs were researched.

One short antenna was found in a R/C catalog that looked interesting. Upon further

Table 7: Receiver Comparison [15]

Parameter	RX72*	Potensky	GWS PICO	RX72-HYB	RX72N-HYB	Garrett
Speed Ctr.	No	No	No	Yes	Yes	No
Channels	4-5	4	4	4	4	4
Weight (gm)	2.4	6.9	6.9	3.5	5.4	4.2
Range (m)	305	305	305	305	305	91
Current (mA)	15		5	15	10	
Voltage (V)	6-10.5		4.8-6	6-10.5	15	
Cost	$125	$89	$45	$125	$127	$86

* Final choice

reading it was found that the antenna was stiff and was 5 inches long. The rules of the competition state that stiff antennas would be figured into the dimensions of the plane. At 5 inches the antenna would certainly affect our maximum dimension, which was not an option.

Professor John R. Hall, the resident pilot and R/C expert at WPI, found instructions to build a homemade short antenna in an R/C magazine. The design was for a short flexible antenna that, according to the competition rules, would not affect the dimensions of the plane. [23]

The normal antenna is just a wire connected to the receiver. This antenna is simply an inductor and small capacitor wired in parallel at the base of the wire antenna. A schematic of the antenna is included as Figure 21. The capacitor and coil effectively tune the receiver to pickup a 72Mhz signal from the transmitter, at a much shorter length than normal.

This antenna was constructed by the group and implemented on the final design. No communication problems were experienced during the operation of the MAV with this antenna. Experiments could be done in the future to see how small this type of antenna could be made before problems are experienced. The antenna drag was reduced greatly by shortening the exposed wire to 1/5 the previous size.

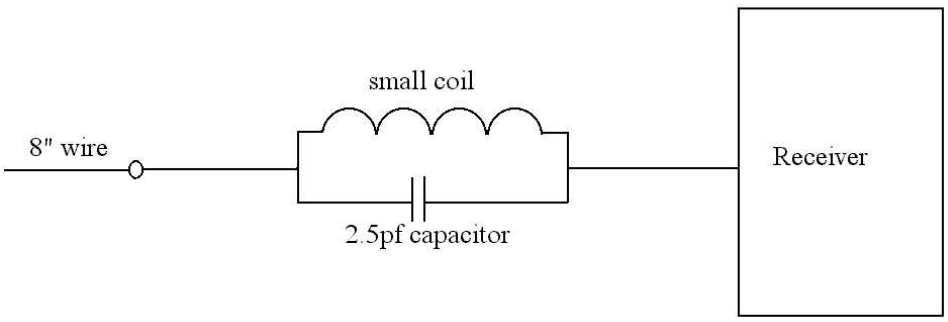

Figure 21: Coil Antenna

6.7 Servos

Servo motors are small electric motors that move the control surfaces of the plane. Servos are plugged directly into the receiver, which powers and controls the servo motors. As with the other components, hobby catalogs were used to find the lightest available models. The lightest servos found were the Wes-Technik 2.4 gram linear servos. The specifications for the servos and a picture are shown as Table 8.

The Wes-Technik servos work quite well but are rather fragile. Several servos were broken during initial flight tests. A 3 gram model of the same design was tested as well and seemed to be much more crash resistant that the smaller servos. The 2.4 grams servos are ideal however and will last if they are mounted and protected adequately.

Table 8: Servo Technical Specifications

Max. deflection (mm)	14
Time to max. deflection (sec)	0.2
Max. output force (gm)	200
Nominal voltage (V)	3-5
Load current (mA)	<100

7 Aerodynamic Analysis

The first step in the analytical process was to determine the vehicle's weight. Since the weight of the individual components were known quantities this was a relatively simple process. If the design had yet to be fabricated only the weight of the structure was unknown. In this case, the structure weight was estimated to be 17% of the total vehicle weight. Note that, for our purposes, the weight of wires, solder, etc. was included in the structure weight. This estimate was based on historical data and later fabrication and testing would validate this estimate. When analysis was performed on fabricated vehicles the measured weight was used.

Wingloading was determined by an analysis of the loiter condition. This analysis yielded a function for the wingloading in terms of the dynamic pressure, the aspect ratio, the Oswald efficiency factor, and the parasitic drag coefficient:

$$\frac{W}{S} = q\sqrt{3\pi A e C_{D,0}} \tag{5}$$

In all cases an Oswald efficiency factor 0.8 was assumed. The aspect ratio, dynamic pressure, and parasitic drag were initially arbitrary values that later converged through iteration. While this did not take into account the various other stages of the vehicle's mission it produced an estimate that was in agreement with historical data.

Knowing the value for the wingloading and the vehicle's weight the required surface area was determined as:

$$S = W\left(\frac{W}{S}\right)^{-1} \tag{6}$$

The dimensions of the vehicle could then be determined based on the pre-defined geometry. The wingspan and chord were determined by iterating the following equations:

$$b = \sqrt{c^2 + p^2 - (\lambda c)^2} \tag{7}$$

$$c = \frac{-2S}{-p - \lambda p + \lambda p - b} \tag{8}$$

The induced drag coefficient is dependent on the lift coefficient. The induced drag coefficient is thus based on the same source (analytical or experimental) as the lift coefficient.

$$C_{D,i} = \frac{C_L^2}{\pi A e} \tag{9}$$

The parasitic drag coefficient was the next quantity to be calculated via one of two ways: A standard component build-up method based on the wing dimensions found above, a fuselage size based on components, and a pre-defined tail area:

$$Re = \frac{\rho V c}{\mu} \tag{10}$$

$$C_f = \frac{0.455}{\log_{10}(Re)^{2.58}} \tag{11}$$

$$FF_{wing,tail} = 1 + \frac{0.6}{x_c} + t_c + 100 t_c^4 \tag{12}$$

$$FF_{fuselage} = 1 + \frac{60}{\left(\frac{l}{d}\right)^3} + \frac{\frac{l}{d}}{400} \tag{13}$$

$$C_{D,0} = \sum_i 2 C_{f,i} F F_i S_{wet,i} \tag{14}$$

The parasitic drag coefficient was found via experimental means by subtracting the

induced drag coefficient from the drag coefficient at the current angle of attack.

$$\begin{aligned} C_{D,0} &= C_D - C_{D,i} \\ &= C_D - \frac{C_L^2}{\pi A e} \end{aligned} \tag{15}$$

The required lift coefficient was found as a function of the vehicle weight, wing surface area, and dynamic pressure:

$$C_L = \frac{W}{qS}$$

Next we found the angle of attack necessary to achieve the required lift coefficient. This was done based on lift coefficient versus angle of attack data for the airfoil. This data was generated via either an analytical method or through experiments. The analytical method utilized thin airfoil theory with finite wing adjustments suggested by Bastedo and Mueller [7].

$$\alpha = \frac{C_L}{\frac{dC_l}{d\alpha}} + \alpha_{L=0} \tag{16}$$

$$\frac{dC_L}{d\alpha} = \frac{dC_l}{d\alpha} \frac{A}{\frac{\frac{dC_l}{d\alpha}}{\pi} + \sqrt{\left(\frac{\frac{dC_l}{d\alpha}}{\pi}\right)^2 + A^2}} \tag{17}$$

The experimental method ustilized curve fits of experimental data for lift coefficient versus angle of attack.

Once the necessary angle of attack was determined a similar process was used to determine the drag coefficient of the airfoil. If an analytical method was used the drag coefficient was found by rearranging Equation 15, where C_L is the previously determined required lift coefficient:

$$C_D = C_{D,0} + \frac{C_L^2}{\pi A e}$$

For the experimental method a curve fit of drag coefficient vs angle of attack data was used.

From this the drag was found as a function of the dynamic pressure, the wing surface area, and the free stream velocity:

$$D = qSC_D$$

Once the drag was known it was necessary to compare it the thrust. First the power output of the motor was determined from the properties of the selected battery and motor system:

$$P = vi - i^2 R$$

The thrust of the propulsion system was determined as a function of the motor power output, the propeller efficiency, and the free stream velocity:

$$T = \frac{P\eta_p}{V} = \frac{(vi - i^2 R)\,\eta_p}{V}$$

For early analytical calculations we had no hard data for the propeller efficiency, nor an analytical solution. So we estimated the propeller efficiency based on historical values. The Black Widow achieved a propeller efficiency of 78% [3]. Based on this, we assumed propeller efficiencies from 60–75%. Later tests demonstrated that the actual propeller efficiencies for the common off the shelf propellers we had access to were closer to 40%.

Finally, the free stream velocity was found:

$$V = \frac{(2P\eta_p\rho^2S^2C_D^2)^{\frac{1}{3}}}{\rho SC_D}$$

This calculated velocity was used to begin the entire analysis iteration again. When the velocity converged the analysis was completed.

Once the analysis had been completed the design was then scored according to Equation 1. The largest dimension was either measured or calculated as:

$$z = \sqrt{c^2 + p^2} \tag{18}$$

Then the endurance was found as a ratio of battery capacity to the current draw:

$$E = \frac{C}{i} \tag{19}$$

Due to the iterative nature of this design analysis a programing tool was developed using the scripting language Python. This program is discussed in more detail in Appendix 11.3.

8 Integration and Fabrication

8.1 Propulsion system

Preliminary static testing was with the WES-Technik DC5-2.5 motor and each of the batteries shown in Table 6 to determine which gave the most thrust with this particular motor. The results showed that the CR2 either alone, or in a set of two or three, gave the most thrust. This is due to the much higher allowable continuous current draw of the CR2. Dynamic testing was conducted with several different battery configurations, gear ratios and propellers. A chart of the dynamic thrust testing is show as Figure 22.

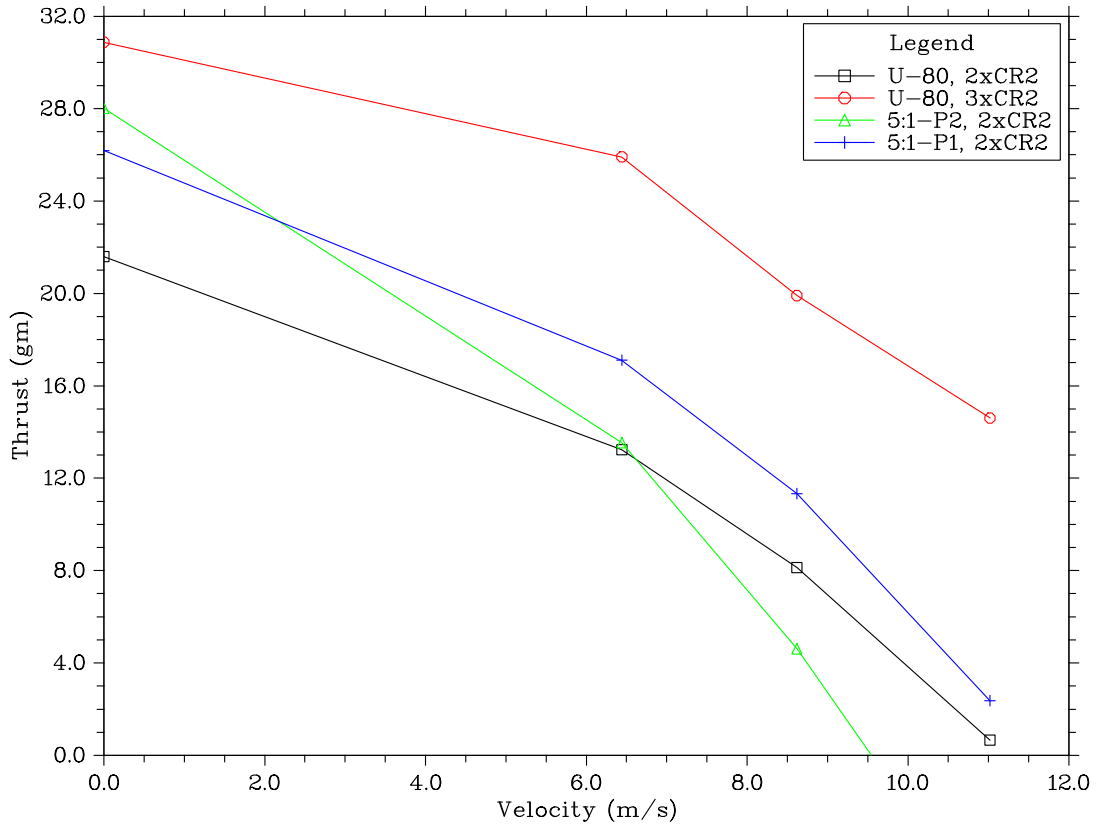

Figure 22: Thrust Comparison

This plot shows that the ungeared motor with 3 CR2 batteries puts out much more thrust than the other configurations. This is of course not without a trade off, three CR2

batteries weighs 50% more than the other configurations. The final design did use three CR2 batteries with the U80 propeller. The added thrust overcame the weight gain of the third battery.

Additionally, the lasso tests described in Section 9.1 were used to gather qualitative propulsion data.

8.2 Controls and Propulsion

If the MAV was to be operated without a speed control the voltage to the receiver needed to be dropped below 5 volts. This was accomplished with a Zener diode for the two CR2 configuration and a voltage regulator for the three CR2 configuration.

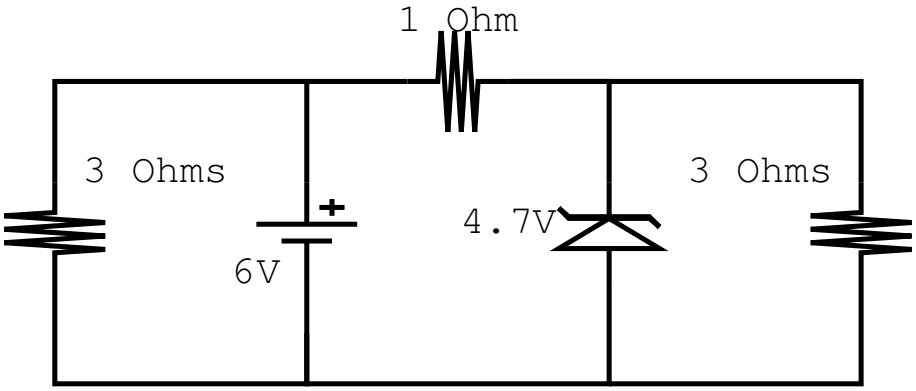

Figure 23: Zener diode circuit

8.3 Structures

There are a few basic qualities that were desired in materials used to build our MAV that we used in the selection of materials. They are:

1. Lightweight — First and foremost the material needs to be very light.

2. Crash resistant — The MAV should be able to survive several crashes before any serious repair is necessary.

3. Structurally sound — The material should be strong enough to maintain its shape during normal flight.

4. Simple to construct — It should be possible to make an entire MAV structure in 4-6 hours.

5. Easy to repair — If damage occurs, it should be possible to fix easily, in order that the most can be learn from each model.

Using these criteria, there were many materials that were experimented with. The old modeling standard, balsa wood, was one of the first materials experimented with. Various plastics were also experimented with including milk jug plastic and overhead transparency film. Polystyrene insulation and packing material was also used for various designs of the MAV.

The preliminary research for building materials showed that polystyrene would be of adequate strength to construct the aircraft out of. This information is from calculations done during A-term 2001 for the preliminary design of the aircraft. This material is the final choice that the team used for the main body of the aircraft. However, another approach had been tried first, which was using transparency film over an arrangement of balsa wood ribs. This can be seen in Figure 3.

This construction method was accomplished by arranging the ribs in a template that held them in place while the transparency was glued over it. The transparency was heated to allow it to flex around the leading edge appropriately and then glued to the rest of the structure. This structure type was found to be quite durable to crashes and also very easy to repair if something did break on it. This structure type was abandoned due to the fact that the construction methods left the final product with many slight imperfections and there was a lack of symmetry, which caused roll problems when it came to flight-testing.

For the final structure, the team decided to implement shaped polystyrene in three sections: a straight center section and two tapered wingtips. The construction methods for all

three of the sections were very similar. The sections were cut to very rough size using a heated wire to cut the foam cleanly. Airfoil cross-sections were cut out of balsa wood and glued to the sides of the foam. The foam was then sanded down to the appropriate size, and then glued together.

This construction method allowed a very symmetrical wing. The underside of the wing was cut hold the components inside the airfoil shape. Tails were fashioned of a balsa wood sandwich with perpendicular grains to increase its rigidity. Because the nose of the plane became thin at the motor mount, the team decided that it was too weak to withstand a crash. As reinforcement, a flat piece of carbon fiber was glued into the structure above the motor. This strengthened the entire leading edge of the wing. Figure 6 shows how the carbon is placed in the construction, the balsa elevons and tails, and the seams where the sections were glued together.

9 Performance Analysis

9.1 Stability

Primary concerns for the MAV were static pitch and roll stability. Dynamic stability was not considered due to complexity, time constraints, and the assumption that static stability would provide acceptable dynamic stability.

9.1.1 Static Pitch Stability Analysis

Static pitch stability was analyzed to ensure that the center of gravity location was such that a disturbed MAV would return to level filght. The free body diagram in Figure 24 shows that the center of gravity must be located in front of the neutral point.

The following analytical process was used to determine the stability of the MAV in the early design stages:

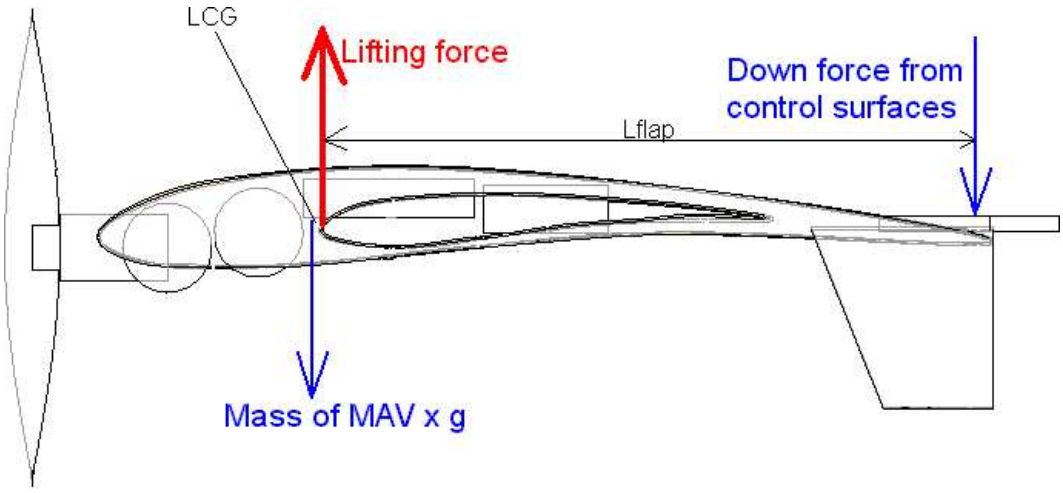

Figure 24: Stability Free Body Diagram

1. The neutral point for the aircraft was determined. For a flying wing the neutral point is the aerodynamic center, which, in our case, was originally assumed (and later experimentally verified) to be located at the quarter chord point.

$$\begin{aligned} \frac{dC_{M_{CG}}}{dC_L} &= 0 \\ x_{CG} - x_{AC_W} &= 0 \\ x_{NP} - 0.25 &= 0 \\ x_{NP} &= 0.25 \end{aligned}$$

2. The forward-most allowable point for the center of gravity was found by:

$$\begin{aligned} -\frac{dC_{M_{CG}}}{dC_L} &= 0.015 \\ -x_{CG} + x_{AC_W} &= 0.015 \\ -x_{MF} + 0.25 &= 0.015 \\ x_{MF} &= 0.245 \end{aligned}$$

3. Pro/Engineer was used to determine the center of gravity via a statics analysis. Or the analysis was done using the following equation and the free body diagram in Figure 24 (all lengths are measured from the leading edge):

$$CG = \frac{M_p x_p + M_m x_m + 2M_b x_{b,1} + M_b x_{b,2} + M_r x_r + 2M_s x_s + M_f x_f + M_t x_t + M_{mis} x_{mis} + M_s}{M_{tot}}$$

4. Finally, the center of gravity was check to insure it was located within the static margin (between the neutral point and the most forward point):

$$x_{MF} \leq x_{CG} \leq x_{NP}$$

For later, fabricated MAVs, the center of gravity location was found via an experimental method:

1. The centerline of the MAV was marked.

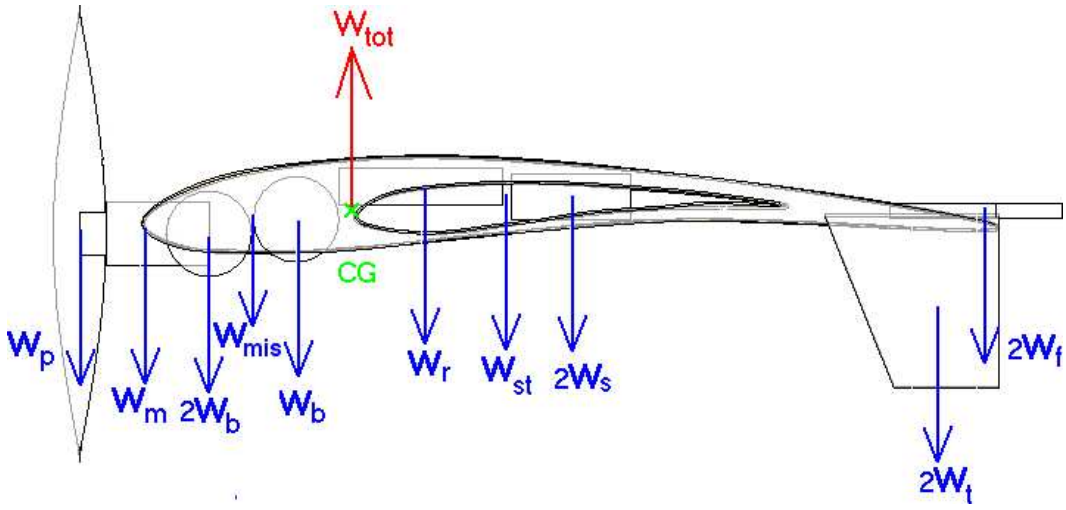

Figure 25: Center of Gravity Free Body Diagram

2. A one meter string was attached to the MAV wingtip at the neutral point (quarter-chord).

3. A plumb bob was attached to the other end of the string.

4. The middle point of the string was elevated such that both the plane and the plumb bob were suspended.

5. The center of gravity was marked as the point were the plumb bob intersected the centerline.

The static margin found in the analytical process was then verified by a lasso test:

1. A 5 meter string was attached to the MAV wingtip at the center of gravity.

2. The propulsion system is started and the controls checked.

3. The MAV, restrained by the string, is flown in circles.

There are two primary goals of the powered lasso test. First, is to test whether or not the plane has enough thrust and lift to fly. Second, to test whether or not the plane is pitch stable. Other, secondary goals are testing control surface area, and trim point.

If the plane is trimmed incorrectly or is vastly unstable the plane will not fly in circles. The trim should be adjusted until the MAV flies level. If level flight could not be acheived the center of gravity position was moved and elevator positions were adjusted. In addition, control surface size was optimized to ensure that the elevators were large enough to provide the required down force.

Lasso tests were also used before each free flight test session to set the trim point for the control surfaces. This was done by putting the MAV on a lasso and adjusting the trim point on the R/C transmitter until the plane flew stable and level without input

9.1.2 Roll Stability

Roll instabilities are caused by fabrication and weight placement asymmetries. Free flight tests were used to test for roll stability. In order to conduct a free flight test the plane would be turned on, the controls checked, and then the MAV would be launched into the air by hand. The pilot would then attempt to keep the MAV in the air. All present parties would keep strict attention on the plane in order to diagnose any problems. Most free flight tests only last 2 seconds. Free flights were a very iterative process. If the MAV rolled to one side the flaps would be trimmed to stop that roll, and the plane re-flown.

Often elevator trim was not enough to produce level flight. If the elevons were too small or to close to the centerline of the plane, the plane would fly straight, but the pilot will not be able to correct a roll or turn the MAV reliably. The vertical tail size and location were also tested with free flights. Each free flight was timed, and some were video taped to be viewed in detail after the test.

The construction materials were also tested quite thoroughly with free flight tests because all flight tests end in a crash. The MAV was inspected closely after each crash for any damage, and the group paid attention to how many crashes each construction method could withstand before the plane was not structurally sound.

9.2 MAV-3

MAV-3 was the first design to feature a polystyrene wing and to perform several flight tests. It had a wingspan of 14cm and a chord of 10.5 cm, with a twin tail and center mounted airlerons. Propulsion was provided by an ungeared DC5-2.4 with a U-80 propeller. This system provided 8 grams of thrust and a flight velocity of 8 m/s. The plane's longest flight was four seconds. This was limited by a lift and thrust deficit. This can be seen form the post-flight testing summarized in the following Figures 26 and 27.

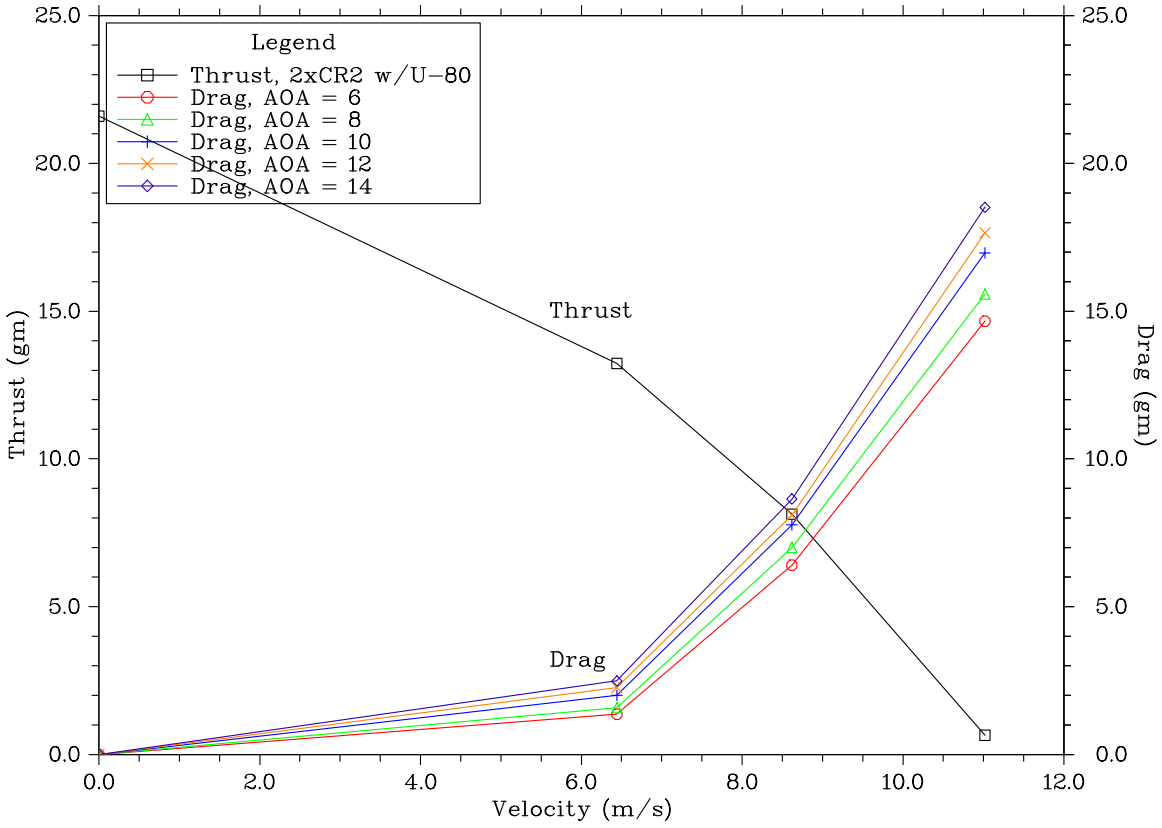

Figure 26: MAV-3 Thrust-Drag

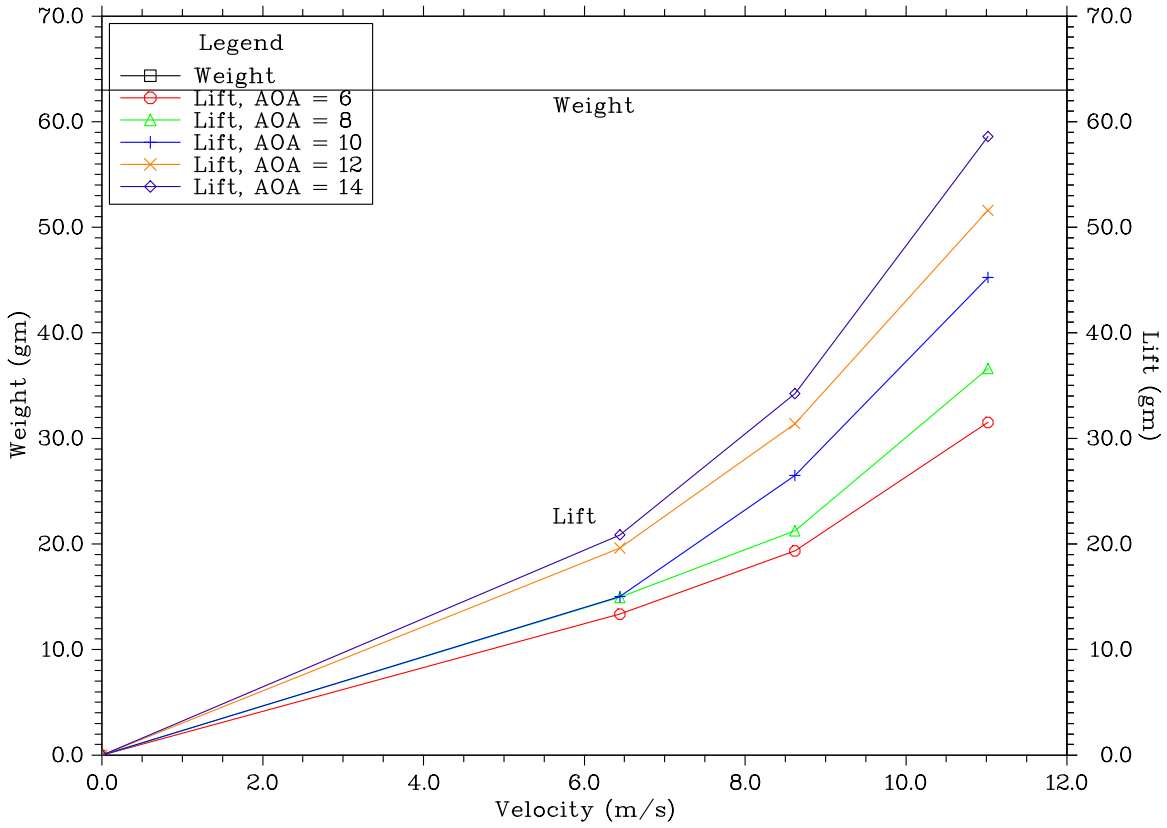

Figure 27: MAV-3 Lift-Weight

9.3 MAV-4

MAV-4 was the final and most successful design produced by the group. As stated earlier, MAV-4 exhibited a two-fold increase in wing area and an aspect ratio change from 1.6 to 1.7. MAV-4 had the same basic tail, elevon, and component configuration as the other design. Initial flights of MAV-4 were conducted with two CR2 batteries and acheived several 5–6 second flights. These flights indicated that the plane was not producing enough lift. It was determined that this was due to a thrust shortfall and the resulting slow flight speed. A third CR2 was added to increase the power output of the propulsion system. This allowed MAV-4 to complete several flights of 10–15 seconds. During these flights the plane was able to climb, however, there was not enough control to perform other maneuvers. This was attributed to the placement of the elevons too close to the centerline.

The group performed a post-flight analysis to ascertain actual performance parameters. MAV-4 was tested in the wind tunnel for lift and drag values. Drag values were combined with propulsion testing to create the thrust-drag plot in Figure 28. This plot shows that flight should be possible between 9 and 12 degrees angle fo attack, and between 9.5 and 11.5 m/s. When this information is combined with Figure 29, a lift-weight plot for MAV-4, it can be determined that the successful design flew at an angle of attack of 9 degrees and velocity of 11.5 m/s.

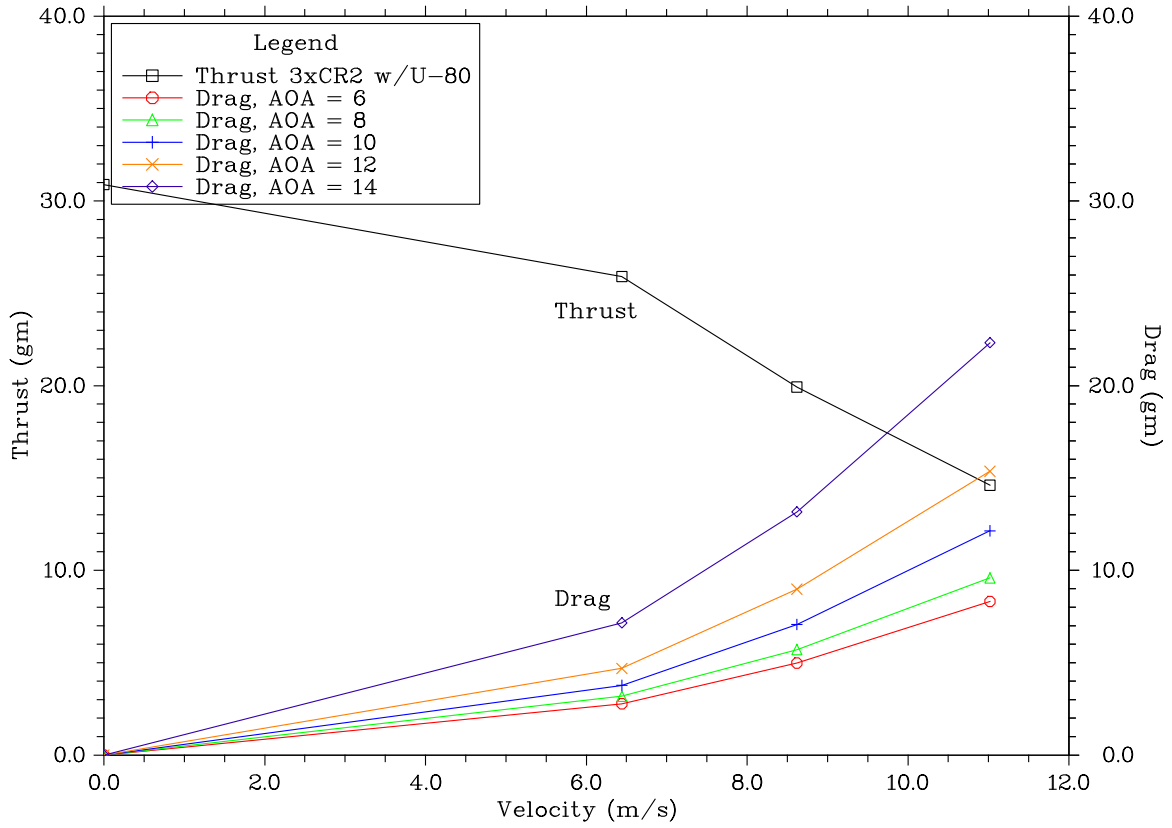

Figure 28: MAV-4 Thrust-Drag

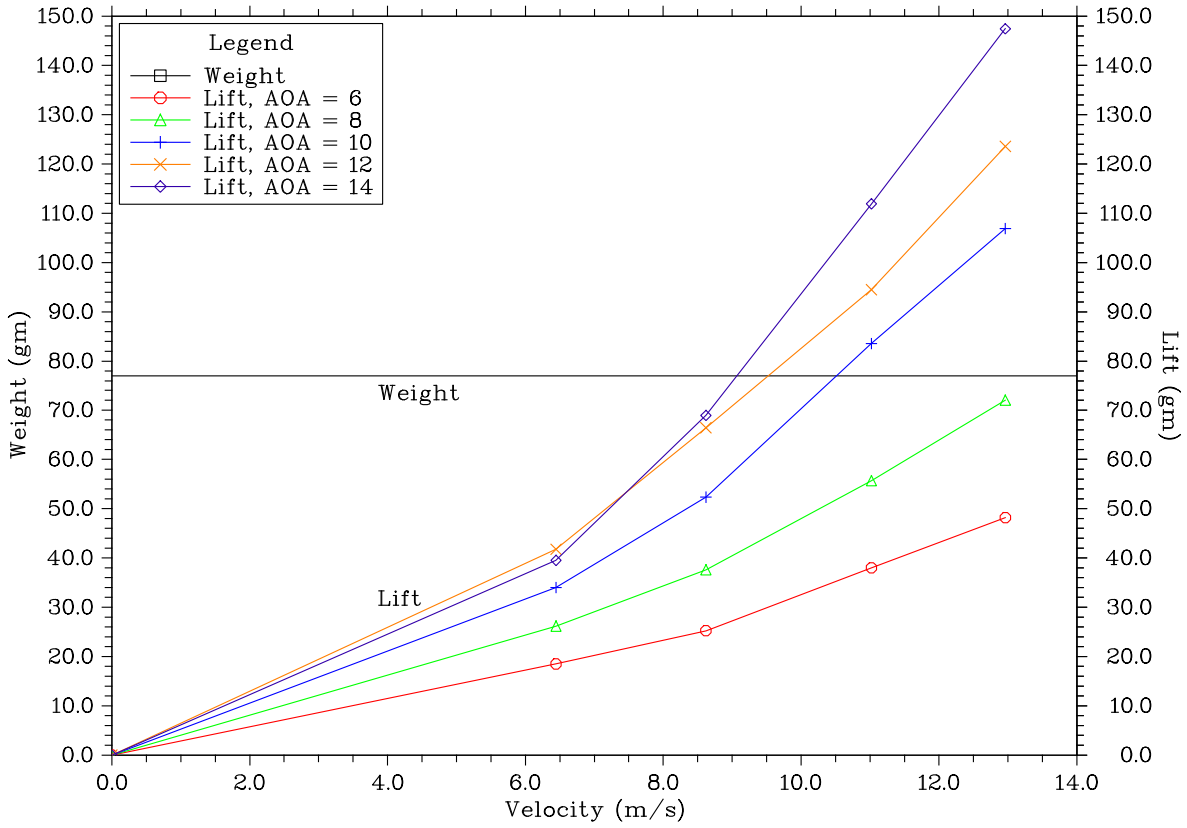

Figure 29: MAV-4 Lift-Weight

10 Conclusions and Recommendations

10.1 Controls

Throughout the design process the designs were plagued with control problems. This was due to several factors. First, the group budgeted too little time to resolve control problems due to our underestimation of control difficulties. Second, the servos utilized for the design were sensitive to torques placed on them by the linkages to the elevons and were fragile. Finally, our control placement could be improved.

Initially the servo linkages to the elevons were constructed of a flexible wire. This method allowed easy modification of the linkages and allowed some of the shock from crash landings to be absorbed by the wire instead of transmitted to the fragile servos. However, flexible links often caused slight torques on the servo track that caused the servos to stick. Thus, a rigid linkage system was used that had the unfortunate consequence of transmitting forces directly to the servos, though they did operate properly.

The main problem with the WES-Technik servos is their durability. Several of the servos were broken on multiple occasions and flight tests were interrupted. The servo motors need to be protected from direct impact and mounted to the plane securely such that a crash will not knock them out of the plane. Also, the flaps should be protected so that any direct impact on the flap will not transfer down through the linkage and break the track that the link attaches to. Repair is possible with these servos, but several attempts are needed in order to understand how the repairing should be done.

In hindsight our choice of servos was the correct one but greater care should have been given, earlier on, to their protection. Their benefits included: their light weight and their linear mechanical output. The linear servo with a simple linkage to the flaps allows the servos to be farther forward in the plane. This is, of course, is crucial for the center of gravity and stability of the plane. Rotary servo motors would be more difficult to use for this size plane because of the CG issues. Also, the linkage design would be much more

complicated because of the geometry of rotary servo motors.

The main problem with MAV-4 in flight was that it could not recover from a roll of any more than about 20 degrees. This was mostly due to the fact that the flaps on the MAV were directly on either side of the center line of the plane. If the flaps were moved to the outside corners of the wing, roll control would be improved. The flaps could easily have an angled pivot axis to not effect the maximum dimension.

Another problem with the MAV rolling is that the lift vector of the plane obviously moves by the same angle. This means that not as much lift is counteracting gravity and the plane will slide from the sky. In this application we were minimizing the size of the craft, which meant that we maximized the wing loading of the craft. Due to this, however, we magnified the effect of the lift vectors changing angle and losing lift.

A better control system may be to have one main elevator and a rudder. With this system the plane would have one flap that would be in the center of the plane to climb, and a rudder. If this were implemented the plane would not have to roll in order to turn; the rudder would produce the yaw necessary to turn. This type of design would allow the plane to be smaller with less of a safety factor in the wing loading to protect against the changing lift vector.

10.2 Airfoil and Geometry

During the later part of the project with a flight deadline approaching the design process was left slightly and an experimental problem solving approach was taken. Therefore, when MAV-3 did not have enough lift the next plane was built much bigger. MAV-4 has an area twice the size of MAV-3, much more than necessary. With extra size comes extra weight and extra drag. The next design by this group would be somewhere in between the two designs in size. This should minimize the drag and allow the plane to fly slightly faster which would provide more lift.

The airfoil that was chosen, the Wortmann FX60100, definitely seemed to be the right

choice for the design. The lift to drag ratio for the wings tested was higher than that of many historical designs, and if the plane had just a slight amount more thrust the MAV would have had plenty of lift for flight. One possible way to add a bit more thrust may be to change the wing geometry slightly. If the wing was swept just slightly to allow more space between the propeller and wing, the propeller may produce more thrust. The motor could also be mounted further out of the wing to produce the same effect. Also, more effort could have been spent on decreasing the drag caused by the airfoil shape and construction methods.

If more time were available, the group would also have tested the effect of dihedral on the flight quality of the plane. The vertical tail size would have been optimized as well, although there was no real problem with the final tail size.

Future projects are already planned to study the behavior of low Reynolds number flows over low aspect ratio wings. It is hoped that the results of these studies will improve our understanding of the effects of wing geometry on performance.

10.3 Propulsion

The propeller used on the final design of the plane was only about 40% efficient. While the plane did fly, this type of inefficiency is unacceptable for MAV design. When the purpose of the design is to be as small as possible, the efficiency of the systems at work is the most important parameter. One of the main items that could have been done differently in this project would be to understand and implement a propeller with higher efficiency, or the use the current propeller in a more efficient manner.

This is the crux of the problem however, because the motor and batteries directly affect the performance of the propeller. When off the shelf components are used for the design it is very hard to find a set that will work together as an efficient system. Real gains could be made if one component of the system could be custom designed. Either a propeller optimized for a motor-battery combination, or a custom battery for a motor-propeller com-

bination that would produce the correct prop speed.

We recommend that future MQPs investigate ways of increasing the efficiency of micro propellers.

10.4 Stability

The center of gravity is of utmost importance to the flight characteristics and overall performance of the plane. As discussed earlier, the center of gravity of the plane needs to be just slightly in front of the quarter-chord point. The final MAV design had a CG about 2mm in front of the quarter-chord, and great pains were taken to keep every component as far forward as possible. On the next model some components would be put even further forward in order to have more freedom to move other components back if necessary. It should also be noted that if the wings were swept back the center of lift would be moved back as well and more pitch stability could be gained, it would, however, be more difficult to store components in the reduced forward section of the wing.

To avoid crashing the aircraft regularly, another method can been used to determine the roll stability. This involves using a force balance which can measure roll moments. Though the materials and tools were available, time did not allow for our group to setup this experimental tool.

10.5 Testing

Another thing the group has learned about a project of this type is to understand testing equipment fully. Early on testing was done in the wind tunnel on several wings but the data was irregular and useless. It was later discovered than there was a physical problem with the setup, but several weeks of testing were lost because it was assumed the force balance was temperamental. The group has learned that it is important to know your equipment so that you know when it is temperamental and when it is not working properly. As much information as possible should be gained from previous students who have used the tunnel

first hand. Gathering useful data is very important and knowing the testing equipment well is the only way to accomplish that.

We recommend that the testing equipment in the aero lab be improved as follows: The current data acquisition box allows only the measurement of lift or drag; both should be monitored at the same time. The interdependence of the force balance should be further examined and either fixed or accurately accounted for. It would be useful to construct a testing apparatus that allows the angle of attack to be set accurately. The majority of the data gathering process should be automated. Software and hardware should be developed to control and monitor the wind tunnel and the test models angle of attack. The data collection and analysis process should automatically convert, store, and provide visualization of the data.

10.6 Design Process

Late in the process the group left analytical analysis in order to do physical problem solving on the plane and its flight. This is necessary on some level because the theory behind MAV design is not fully developed and nothing can be modeled totally realistic anyways. However, the group has reached the conclusion that analytical analysis should not be left fully; it should be used to supplement physical testing and to help analyze problems. With a group of 4 people as we had, there should be time for both analytical and testing work at the same time. As mentioned above, at one point the group decided to scale the model up, but without any analytical analysis on the size issue, the plane was made too big and still would not fly. Subsequent testing has shown that a size somewhere between MAV-3 and MAV-4 would be optimal for our component system.

The group has also noticed that the some of the choices made during the design process should have been more influenced by past MAV designs than they were. The elevon/rudder combination that was discussed, for example, was used by the very successful Black Widow design. It would have been useful to understand why they used that design early on, because

it makes perfect sense for a design of this sort.

The group also wanted to note that when projects are completed with products from industry, students should always remember they are in the real world. When buying products there is always a lead time to get the item, and that time is generally larger than expected. When there are items that need to be tested for the use in decision-making, such as motors, they should be purchased as soon as they are considered a possible candidate. Any waiting that is done will be magnified when the deadline approaches. This group had some problems with breaking components, and lead times disrupted testing progress greatly, which in the end, kept the group from being ready for the MAV 2002 competition.

We recommend that future projects pursue analysis and experimental testing in parallel, and continually view the results in perspective with historical norms. Also, it is essential to obtain physical components for testing early on to verify early analytical predictions.

References

[1] Hughes, Austin. Electric Motors and Drives: Fundamentals, Types and Applications, 2nd Edition.

[2] MAV Competition 2002. Available: http://meweb.et.byu.edu/mav/rules/index.html [22 Apr. 2002].

[3] Grasmeyer, Joel M. and Keennon Matthew T. Development of the Black Widow Micro Air Vehicle. AIAA-2001-0127.

[4] Mueller, Thomas J. Aerodynamic Measurements at Low Reynolds Numbers for Fixed Wing Micro-Air Vehicles.

[5] Morris, Stephen J. Design and Flight Test Results for Micro-Sized Fixed-Wing and VTOL Aircraft.

[6] Torres, Gabriel and Mueller, Thomas J. Micro Aerial Vehicle Development: Design, Components, Fabrication, and Flight-Testing. Available: http://www.nd.edu/~mav/auvsi/torres.htm.

[7] Bastedo, Jr., William G. and Mueller, Thomas J. Performance of Finite Wings at Low Reynolds Numbers. Indiana: University of Notre Dame.

[8] Raymer, Daniel P. Aircraft Design: A Conceptual Approach, 3rd Ed. Reston: AIAA, 1999.

[9] WES-Technik. Coreless Motors. Available: http://wes-technik.de/English/motors.htm [9 April 2002].

[10] RMB. Special Precision Motor 8mm SYV88001. Available: http://smoovy.com/products/SYV88001.htm [9 April 2002].

[11] Faulhaber. DC-Micromotors Series 1224 ... S. Available: http://www.micromo.com/images/1224_7.PDF [9 April 2002].

[12] Faulhaber. DC-Micromotors Series 1319 ... S. Available: http://www.micromo.com/images/1319_7.PDF [9 April 2002].

[13] Powerstream Technologies. Available: http://www.powerstream.com/ [7 April 2002].

[14] McMichael, James M. and Francis, Michael S., Col. USAF (Ret.). Micro Air Vehicles - Toward a New Dimension in Flight. Available: http://www.darpa.mil/tto/MAV/mav_auvsi.html [14 September 2001].

[15] Sky Hooks & Rigging. Micro SHR-RX72 Receivers. Available: http://www.microrc.com/RV-RX72.htm [9 April 2002].

[16] University of Florida MAV Site, Last Modified: 17 Dec 99, Available: http://www.aero.ufl.edu/~issmo/mav/mav.htm

[17] Notre Dame Micro Aerial Vehicle Development Group, Available: http://www.nd.edu/~mav/

[18] BYU MAV Site, Available: http://www.me.byu.edu/mav/

[19] Arizona State University MAV Competition 2000, Available: http://www.eas.asu.edu/~uav/main.html

[20] Design of Micro-Aerial Vehicle, Blondin, Sean M, I DeBarros, M Falcone, D Henry, K McWilliams, S Seney, J Wong, WPI MQP, 2001

[21] Lowry, Dr. John T.; Propeller Aircraft Performance and The Bootstrap Approach; ALLSTAR Network, Copyright 1999. Available: http://www.allstar.fiu.edu/aero/BA-Background.htm [3 April 2002].

[22] NASG Airfoil Database. Available: http://www.nasg.com/afdb/index-e.phtml [17 Sept 2001].

[23] Worth, John. “Short Antennas.” RC MicroFlight.com, September 2001. Available: http://www.rcmicroflight.com/sep01/cloud9_1.asp [10 Feb 2002].

[24] Fillipone, A. Aerodynamic Drag: Speed Related Drag. “Drag at Very Low Speeds” (1999-2002). Available: http://aerodyn.org/Drag/speed-drag.html.

[25] Laitone, E. V. “Aerodynamic Lift at Reynolds Numbers Below 7×10^4 ,” AIAA Journal, Vol. 34, No. 9, Sept. 1996.

[26] Mueller, T.J. and Torres, G.E. "Aerodynamic Characteristics of Low Aspect Ratio Wings at Low Reynolds Numbers," Fixed and Flapping Wing Aerodynamics for Micro Air Vehicle Applications. Ed. Thomas J. Mueller. AIAA: Virginia, 2001. 115-141.

[27] Ramamurti, R. and Sandberg, Wm. "Computation of Aerodynamic Characteristics of a Micro Air Vehicle," Fixed and Flapping Wing Aerodynamics for Micro Air Vehicle Applications. Ed. Thomas J. Mueller. AIAA: Virginia, 2001. 537-555.

[28] White, F.M. Fluid Mechanics. Fourth Ed., WCB/McGraw Hill: Boston, 1999. 460.

11 Appendices

11.1 Force Balance Independence

It was suspected that the lift and drag measurements of the force balance were not independent. To test this hypothesis four cases were tested: while measuring drag, a drag and then a lift force were applied and while measuring lift, a lift and then a drag force were applied. It was observed that applying a lift force had no effect on the drag force measurement. However, applying a drag force while measuring lift displayed a noticeable linear trend that is significant when compared to the measured lift force when a lift force is applied.

All measurements were made with LabVIEW in conjunction with the silver box and force balance. Measurements were conducted in four cases detailed below:

1. The DAQ box was set to measure drag.The force balance was mounted on a calibration stand outside the wind tunnel and a drag force was applied as shown in Figure 30.

Figure 30: Drag force applied

2. The DAQ box was set to measure drag. The force balance was mounted in the wind tunnel and a lift force was applied as shown in Figure 31.

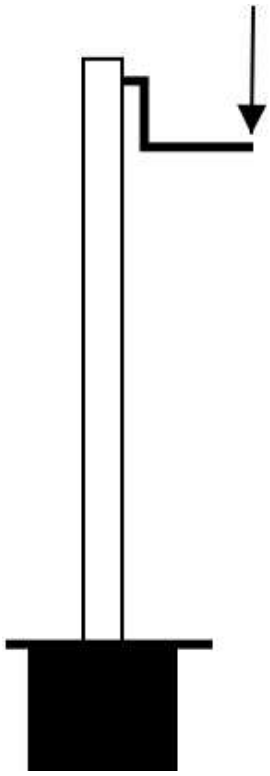

Figure 31: Lift force applied

3. The DAQ box was set to measure lift. The force balance was mounted in the wind tunnel and a lift force was applied as shown in Figure 31.

4. The DAQ box was set to measure lift. The force balance was mounted on a calibration stand outside the wind tunnel and a drag force was applied as shown in Figure 30.

The results are shown in the following two charts. One shows the results from steps 1 and 2 above and the other from steps 3 and 4. The results show that a drag measurement is independent of an applied lift force. However, a lift measurement is dependent on the applied drag force. Note that error bars are plus and minus one standard deviation and the y-intercepts of trends have been adjusted to allow comparison.

11.2 Testing Procedures

11.2.1 Drag Calibration

1. Remove the force balance from the wind tunnel

2. Attach the force balance to the lexan mount so that the balance beam is horizontal

3. Attach a parachute so it hangs down from the sting on the force balance

4. Take a labview measurement of the drag recording it into a spreadsheet file

5. Add weight to the parachute and take another measurement recording it into a spreadsheet file

6. Repeat step 5 from 1 gram, varying weights of about 5 grams each time, to more than the maximum force that should occur from the testing, an easy way to do this is to calibrate to more weight than the test model itself

11.2.2 Lift Calibration

1. Place the force balance back into the wind tunnel and attach the test model on it so that the forces are all down
2. Take a zero measurement and record the data onto a spreadsheet file
3. Add weight to the top of the wing as close to the center as possible, and as close to the center of lift as possible also
4. Take a measurement and record it onto a spreadsheet file
5. Repeat steps 9 and 10 from 1 gram with varying weights of about 5 grams until you have a larger range than will ever be generated

11.2.3 Propulsion Testing

1. Calibrate the force balance for drag.
2. Move the force balance to the tunnel to take dynamic thrust measurements.
3. Wire the motor so that we can measure the voltage, current, and thrust output by the batteries or the motor.
4. Run the tunnel at 7.5, 10, and 13 Hz., which equal 6.4, 8.6, and 11 m/s respectively.
5. Repeat steps 4 for the following setups:
    (a) Micro DC5-2.4 Direct Drive U-80 prop
        i. 2xCR2
        ii. 3xCR2
    (b) Micro DC5-2.4 5:1 Gear ratio with 2 CR2
        i. P1 propeller

ii. P2 propeller

iii. Carbon propeller

11.2.4 Lift and Drag Testing

1. Set the DAQ box to read lift and calibrate for lift.
2. Set the tunnel velocity to one of: 7.5, 10, 13 Hz (6.4, 8.6, 11 m/s).
3. Take measurements at 12 different approximate angles of attack: (-4, -2, 0, 2, 4, 6, 8, 10, 12, 14, 16, 18). Take a zero measurement at zero tunnel velocity between each measurement.
4. Repeat steps 2 - 3 for the remaining tunnel speeds.
5. Set the silver box to read drag and calibrate for drag then repeat steps 2–4 for the following setups:
   (a) MAV-3
   (b) MAV-4
6. Repeat for drag.

11.3 Codes

11.3.1 Aerodynamic Analysis

For the aerodynamic analysis portion of this project, code was develped to follow the previously mentioned iterative process. The current version is available at:

http://francisbarnhart.com/projects/mqp/code/